

Study on the Underlying Mechanism of Yinhuo Gout Granules in the Treatment of Gouty Arthritis by Integrating Transcriptomics and Network Pharmacology

Qiang-qiang Fan¹, Bing-tao Zhai¹, Dan Zhang¹, Xiao-fei Zhang¹, Jiang-xue Cheng¹, Dong-yan Guo¹⁻³, Huan Tian⁴

¹School of Pharmacy, Shaanxi University of Chinese Medicine, Xi'an, 712046, People's Republic of China; ²Shaanxi Key Laboratory of Chinese Medicine Fundamentals and New Drugs Research, Shaanxi University of Chinese Medicine, Xi'an, 712046, People's Republic of China; ³State Key Laboratory of Research & Development of Characteristic Qin Medicine Resources (Cultivation), Shaanxi University of Chinese Medicine, Xi'an, 712046, People's Republic of China; ⁴Xi'an Hospital of Traditional Chinese Medicine, Xi'an, 712046, People's Republic of China

Correspondence: Dong-yan Guo; Huan Tian, Email 2051080@sntcm.edu.cn; 18149412681@163.com

Purpose: Yinhuo Gout Granules (YGG) is a traditional Chinese medicine preparation with a variety of pharmacological effects, and its clinical efficacy in the treatment of gouty arthritis (GA) has been fully confirmed. However, the pharmacodynamic basis of YGG and its anti-inflammatory mechanism of action in GA are unknown. The objective of this study was to identify the active components and molecular mechanisms of YGG in the treatment of GA.

Methods: Ultra-performance liquid chromatography-electrospray ionization tandem mass spectrometry (UPLC-ESI-MS/MS) and network pharmacology were used to identify and predict the potential active ingredients and related signaling pathways. Then, we revealed the anti-GA effects of YGG based on pharmacodynamic experiments in GA rats. Finally, we integrated transcriptomics and network pharmacology to elucidate the potential mechanism of action and verified the putative mechanism by molecular docking, immunohistochemical (IHC) and Western blot.

Results: We have identified 10 major active components of YGG that may have anti-GA effects, such as ferulic acid, rutin, luteolin, etc. Using molecular docking, we found that 10 major compounds could bind well to TNF, PTGS2, IL-6, IL1 β , NOS2 and PTGS1, and the binding energies were all less than -5 kcal/mol. Animal studies have shown that YGG can improve joint inflammation and inflammatory cell infiltration, reduce serum UA, BUN and Cr levels ($p < 0.01$), and decrease IL-1 β , IL-6, TNF- α , COX-2 and PGE2 levels in synovial tissue ($p < 0.01$), which are associated with the pathogenesis of GA. IHC and Western blot results showed that YGG could regulate TLR4/MYD88/NF- κ B pathway to inhibit the inflammatory response induced by GA.

Conclusion: This study found that YGG could not only improve the disease of GA by inhibiting the production of UA in the body, but also target the regulation of TLR4/MYD88/NF- κ B signaling pathway through a variety of active components to achieve effective therapeutic effects on GA.

Keywords: gouty arthritis, Yinhuo Gout granules, transcriptomics, TLR4/MYD88/NF- κ B signaling pathway

Introduction

Gouty arthritis (GA) is a common metabolic disease in humans caused by abnormalities in purine metabolism and excessive Uric acid (UA) production.¹ Hyperuricemia (HUA) is the basis for the occurrence and development of GA. During the HUA stage, the UA level continues to increase, leading to the deposition of Uric Acid Sodium (MSU) crystals in and around the joints, and then stimulating the body to produce a large number of pro-inflammatory factors, such as Interleukin-1 β (IL-1 β), Interleukin-6 (IL-6), tumor necrosis factor- α (TNF- α), etc. Eventually induces GA, accompanied by severe pain and acute inflammation.² GA occurs in approximately 1–4% of the general population, and in a few countries, the prevalence is as high as 10%, affecting mainly middle-aged and elderly people and significantly more men

than women.³ In addition, the global incidence of GA is on the rise due to improper dietary habits, inadequate exercise and disorders of metabolism.⁴ Currently, effective treatments for GA include reducing inflammation, lowering UA levels in blood and urine, and dissolving MSU crystals to improve arthritis function. Therefore, in the clinical treatment of GA in western medicine, most of them use combination therapy. On the one hand, drugs such as allopurinol tablets, febuxostat tablets, probenecid tablets, and benzbromarone are used to reduce the production of UA or increase the metabolism of UA in patients.⁵ On the other hand, the use of colchicine, non-steroidal anti-inflammatory drugs (NSAIDs), corticosteroids and painkillers to inhibit articular inflammation in patients with development and ease the pain.⁶ However, long-term use of these drugs may cause adverse reactions such as leukopenia, skin and mucous membrane damage, bone marrow suppression, gastrointestinal tract damage, liver and kidney damage.⁷ Therefore, it is imperative to explore new treatments for GA, especially therapeutic drugs from alternative medicine. GA has been treated in China for thousands of years using Chinese medicine.⁸ Compared with Western medicine, Chinese medicine has the efficacy of multitargeting and treating both the symptoms and the root cause of GA and can control the inflammation of GA in a safer way.⁹

Yinhua Gout Granules (YGG), an in-house preparation of Xi'an Traditional Chinese Medicine Hospital, have achieved good efficacy in the treatment of acute attacks of gouty arthritis. YGG is composed of ten herbs, including *Lonicera japonica* Thunb, *Scrophularia ningpoensis* Hemsl, *Angelica sinensis* (Oliv.) Diels, *Glycyrrhiza uralensis* Fisch, *Rehmannia glutinosa* Libosch, *Paeonia lactiflora* Pall, *Atractylodes macrocephala* Koidz, *Amomum villosum* Lour, *Ligusticum chuanxiong* Hort, and *Dioscorea opposita* Thunb (Table 1). A variety of herbs in YGG have been reported to have significant anti-inflammatory or anti-GA effects. For example, *Lonicera japonica* Thunb has the efficacy of clearing heat and removing toxins, dispersing wind and clearing collaterals, and its active ingredient, rutin, can produce significant anti-inflammatory, antibacterial, antioxidant, and bone and soft tissue repair effects by targeting pro-inflammatory factors such as IL-1 β , TNF- α , and other pro-inflammatory factors.¹⁰ *Scrophularia ningpoensis* Hemsl and *Glycyrrhiza uralensis* Fisch also has the effect of heat-clearing and detoxifying, it contains many kinds of flavonoids ingredients can influence the expression of inflammatory cytokines, which regulate the NF- κ B signaling pathways, in order to realize the anti-inflammatory analgesic effect.^{11,12} In addition, many clinical trials have shown that taking Yinhua Gout granules can significantly relieve the symptoms of gouty arthritis. For example, Bai et al treated 112 patients with gouty arthritis using YGG and diclofenac sodium extended-release capsules, and the results showed that Yinhua Gout granules had a significant therapeutic effect on gouty arthritis.¹³ Zhang et al also found through clinical studies that YGG could effectively treat gout attacks by reducing UA levels in the blood and urine of patients.¹⁴ Lei et al used YGG to study the clinical treatment of 62 patients with GA, and the results showed that YGG could effectively regulate the expression of pro-inflammatory factors (IL-1 β , IL-8 and TNF- α) in patients with GA, improve the inflammatory response, reduce the level of serum UA, and thus improve the symptoms of patients with GA.¹⁵ However, the composition of YGG is very complex. To date, only single herbs or components in YGG have been extensively studied for their anti-GA effects. The overall mechanism of action of multicomponent YGG has not been reported, and it is not known whether the interaction between the components affects the mechanism of YGG in treating GA. Therefore, there

Table 1 The Latin Name, English Name, Chinese Name, and Grams of Herbs in YGG

Latin Name	English Name	Chinese Name	Grams(g)
<i>Lonicera japonica</i> Thunb	<i>Lonicera japonica</i> Flos	Jin Yin hua	30
<i>Scrophularia ningpoensis</i> Hemsl	<i>Scrophulariae</i> Radix	Xuan Shen	30
<i>Angelica sinensis</i> (Oliv.) Diels	<i>Angelicae sinensis</i> Radix	Dang Gui	20
<i>Glycyrrhiza uralensis</i> Fisch	<i>Glycyrrhizae</i> Radix Et Rhizoma	Gan Cao	10
<i>Rehmannia glutinosa</i> Libosch	<i>Rehmanniae</i> Radix	Di Huang	15
<i>Paeonia lactiflora</i> Pall	<i>Paeoniae</i> Radix Alba	Bai Shao	20
<i>Atractylodes macrocephala</i> Koidz	<i>Atractylodis macrocephala</i> Rhizoma	Bai Zhu	20
<i>Amomum villosum</i> Lour	<i>Amomi</i> Fructus	Sha Ren	6
<i>Ligusticum chuanxiong</i> Hort	<i>Chuanxiong</i> Rhizoma	Chuan Xiong	15
<i>Dioscorea opposita</i> Thunb	<i>Dioscoreae</i> Rhizoma	Shan Yao	30

is an urgent need to elucidate the mechanism of anti-GA action of YGG, which will be important to guide the clinical application of YGG.

In recent years, because the systematic and holistic research model of network pharmacology is in line with the characteristics of the holistic concept of Chinese medicine and can be based on the relationship between drug constituents and disease targets revealed through visualization tools, the active components and potential mechanisms of action of Chinese medicine for treating diseases can be better presented.¹⁶ Transcriptomics is widely used for research at the molecular level because of its high throughput.¹⁷ Unlike the theoretical predictions of network pharmacology, transcriptomics takes tissues as the object of study to objectively reveal disease development processes and molecular mechanisms from a practical point of view. Through the integration of transcriptomics and network pharmacology, the precise mechanism of drug action can be more comprehensively elucidated.

In this study, we identified and characterized the main components of YGG by UPLC–ESI–MS/MS. Subsequently, we conducted *in vivo* experiments to evaluate the effect of YGG on GA. In addition, we obtained the weight index of each herb using the principle of YGG's monarch and minister combination as the standard, in conjunction with the OB value and relative content of each constituent, and determined its potential absorption by the blood in theory. Potential active components and mechanisms of action of YGG were predicted by network pharmacological analysis, and we employed molecular docking technology to confirm the binding of YGG active components to their core targets. Transcriptomic approaches were integrated to further explore the mechanism of action of YGG in the treatment of GA. Finally, IHC and Western Blot were used to verify and explore the exact mechanism of YGG anti-GA effect, providing scientific basis for its clinical application (Figure 1).

Materials and Methods

Drugs and Reagents

YGG (20220310) was provided by the Preparation Department of Xi'an Hospital of Traditional Medicine (China). Colchicine (101176) was purchased from the National Institutes for Food and Drug Control (China). Allopurinol

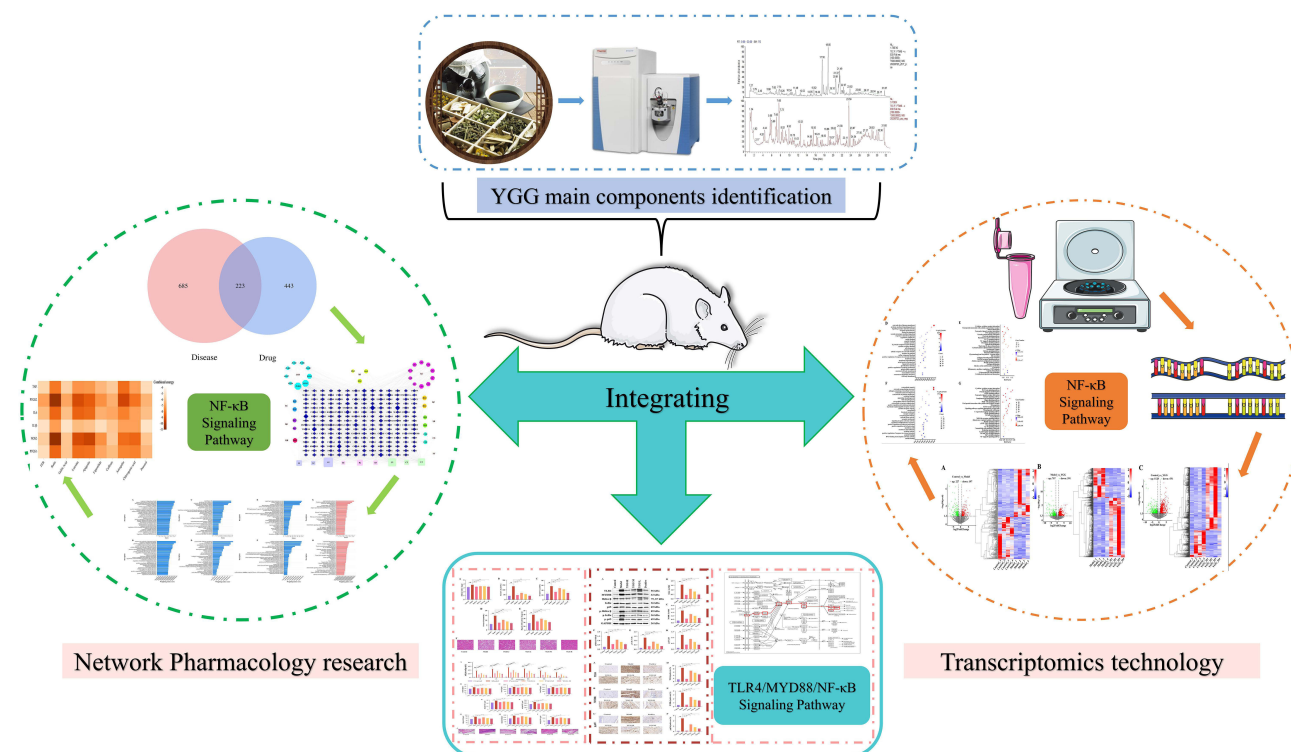


Figure 1 A strategy to obtain more accurate mechanisms by integrating transcriptomics and network pharmacology.

(A800424) was acquired from Shanghai Macklin Biochemical Co., Ltd. (China). Potassium oxonate (PO) (S17112) and MSU (S30775) were obtained from Shanghai Yuan Ye Biotechnology Co. (China). Uric acid (UA) (C012-2-1), creatinine (Cr) (C011-2-1), urea nitrogen (UN) (C013-2-1) and xanthine oxidase (XO) (20220830) kits were obtained from Nanjing Jiancheng Bioengineering Institute (China). ELISA detection kits, including IL-1 β (202207), IL-6 (202207) and TNF- α (202207), were purchased from Shanghai Enzyme Link Biotechnology Co. (China). Primary antibodies against TLR4 (19811-1-AP), I κ B α (10268-1-AP), and p65 (10745-1-AP) were purchased from Proteintech Group, Inc. Antibodies against IKK α / β (ab178870), p-IKK α / β (ad194528), p-p65 (ad76302), and GAPDH (ad8245) were purchased from Abcam, and antibodies against MYD88 (BS-1047R) and p-I κ B α (ET1609-78) were purchased from Huabio (China). The HRP-goat anti-rabbit secondary antibody (SA00001-2) was purchased from Proteintech Group, Inc. (China).

Instrumentation and UPLC–ESI–MS/MS Conditions

UPLC separation was performed using Hypersil Gold C₁₈ (2.1*100 mm, 1.9 μ m). Gradient elution was performed with 0.1% (v/v) formic acid in deionized water (eluent A) and acetonitrile (eluent B). All eluents were filtered, degassed, and stored under pressure. The flow rate was 0.3 mL/min. The gradient elution procedure is shown in Table 2.

Full scan mass spectra were evaluated on a Q-Exactive mass spectrometer by acquisition software. The electrospray ionization (ESI) conditions included a sheath gas flow rate of 45 Arb, an auxiliary gas flow rate of 10 Arb, spray voltages of +3.5 kV and –3.5 kV in positive and negative modes, respectively, a capillary temperature of 275 °C, and an auxiliary gas heater temperature of 450 °C.

The analysis was performed using Compound Discoverer 3.0 software, using the online mz Cloud spectral library and the Thermo Scientific mz Vault spectral library for retrieval in conjunction with available chemical composition information.

Animal Experiment

120 male pathogen-free SD rats (8 weeks old, 200 g \pm 20 g) Chengdu Dashuo Experimental Animal Co., Ltd. (Chengdu, China, licensed ID: SCXK (Sichuan) 2020–030). Each rat was kept in a clean rearing cage at a controlled temperature of 23 °C \pm 1 °C. After 7 days of acclimatization, 120 SD rats were randomly divided into 6 groups as follows: the control group, the model group, the positive group, the YGG-L group, the YGG-M group, and the YGG-H group, with 20 rats in each group. Except for the control group, the rats in each group were intraperitoneally injected with 300 mg/kg potassium oxonate suspension for 14 consecutive days to simulate the symptoms of elevated UA levels in the GA rat model. From Day 12, except for the control group, 0.1 mL of MSU suspension at a mass concentration of 25 mg/mL was injected into the right ankle joint at 45° into the medial tibial tendon with a sterile syringe, 3 days in a row.¹⁸ Contralateral joint capsule protrusion and the appearance of redness and swelling in the joint were considered to be the criteria for a successful injection. During the experiment, equal volumes of saline were administered by gavage to the control and model groups, 10 mg/kg allopurinol and 1 mg/kg colchicine were given to the positive group, and YGG were administered once daily to the drug delivery group at different concentrations for 14 consecutive days. The dose for rats was 10 mg/kg by gavage. At the end of the experiment, all rats were anesthetized with 3% pentobarbital

Table 2 Gradient Elution Table

Time	0.1% Formic Acid in Deionized Water(%)	Acetonitrile(%)
0	98	2
1	98	2
15	60	40
25	2	98
30	2	98
33	98	2

intraperitoneally injected, and serum and related tissues were collected. During this period, all rats were allowed free access to water and food.

Biochemical Sample Collection and Analysis

On Day 14, 1 h after the end of drug administration, the abdominal aortas of the rats were punctured for blood under anesthesia. All blood samples were placed at room temperature for 1 h and centrifuged at 4 °C and 3000 r/min for 10 min. The serum was isolated and then kept at -80 °C. Immediately after death of the rat, the right ankle joint was excised and incised along the median to expose the ankle joint cavity, and the synovial tissue peripheral joint capsule and surrounding soft tissues were removed. In a 4% paraformaldehyde solution, the yellowish synovial tissue from the joint cavity was extracted and fixed. Bilateral kidneys were quickly removed on an ice table, blotted dry on filter paper, weighed on an electronic analytical balance, and the kidney coefficients were calculated. The right kidney tissue was fixed with 10% paraformaldehyde and prepared for use, while the left kidney tissue was stored in lyophilized tubes at -80 °C until analysis. A 10% liver tissue homogenate was prepared by mixing liver tissue (100 mg) from each rat with cold saline solution (900 µL). All homogenized samples were centrifuged at 4 °C and 3000 r/min for 10 min. The supernatants were transferred and stored at -80 °C until analysis.

ELISA kits were used to measure the levels of TNF-, IL-1 β , IL-6, COX-2, and PGE2 in accordance with the manufacturer's standard protocol. UA, Cr, UN, and XO assay kits were purchased from Nanjing Jiancheng Institute of Biological Engineering, and serum and liver biochemical tests were performed according to the corresponding manufacturer's instructions.

Evaluation of Ankle Swelling in Rats

The increase in the diameter of the right ankle joint was considered an indicator for the evaluation of gouty arthritis. A marker was used to mark the same position on each rat to ensure that the calipers were measuring at the same position. Right ankle swelling was considered the difference between the basal value before MSU suspension injection and the detected values observed at different time points (0, 2, 6, 12, 24, 36, 48 h) after MSU suspension injection. That is, [ankle detected value (mm) - ankle base value (mm)]/ankle base value (mm) × 100%. To ensure the results were as accurate as possible, the entire measurement process was carried out by a single experimenter to reduce unnecessary human error.

Histopathological Evaluation of the Kidney and Synovium

Fresh synovial and renal tissue was embedded in a decalcifying solution for three days after being treated with 4% paraformaldehyde. Subsequently, wax tissue blocks were cut into sections, and hematoxylin-eosin (HE) staining was carried out using paraffin-embedded Carrier slides in accordance with a set methodology. Histological images of the kidney and synovium were recorded by a panoramic section scanner.

Network Pharmacology Analysis

YGG Component Attribution

To attribute and screen the components of YGG, we screened and attributed the components obtained from UPLC-ESI-MS/MS analysis using a database search of the Traditional Chinese Medicine Systematic Pharmacology Database and Analysis Platform (TCMSP). Oral bioavailability (OB) \geq 30% and drug-likeness (DL) \geq 0.18 were employed as screening criteria. In addition, to ensure that all components of YGG were fully considered, we reviewed the literature reports of all medicinal herbs included in YGG, and the components that were clearly reported were also included in the main components of YGG. Finally, all the components were attributed to the original herbs contained in YGG to obtain the main components of YGG.

Antigout Target Prediction of YGG

Using the TCMSP, Herb and PDB databases, all drug component targets were retrieved. All disease targets associated with GA were obtained using the CTD, OMIM and Gene Cards databases. These database results were aggregated, and

duplicate items were removed. Subsequently, the action target of YGG was localized to the GA action target, and the potential target of the anti-GA action of YGG was obtained.

Establishment of the YGG Weighting Index

YGG is made up of a wide variety of bioactive components, but the relative contents of each active component found in YGG are notably different from one another. Oral bioavailability (OB) is an essential determinant of the pharmacokinetic process and in vivo drug properties. YGG is an herbal compound consisting of 10 herbs, and the principles of its monarch and minister are also important parameters in the treatment of diseases.

First, we used the AHP method to determine the importance of each component in the compound using the compound monarch as the criterion and combining the pharmacological effects of each component in the literature. Then, the weight index X_i of each component was obtained by the SPSSPRO online data analysis platform. Finally, to more clearly illustrate the significance that major active components play in the pharmacological mechanism, we established the relationship between YGG monarchs and ministers, the relative content of each component, and the oral bioavailability:¹⁹

$$C_i = R_i \cdot O_i \cdot X_i$$

The relationship shows that C_i represents component I, R_i represents the relative content of component I in the total composition, O_i represents the oral bioavailability of component I, and X_i represents the weighting index of component I.

$$T_i = \sum_{i=1}^n C_i$$

The relationship shows that T_i denotes the corresponding target sum of component I.

$$P = (T_0 + T_1 + T_2 + \dots + T_n)$$

The sum of the corresponding objectives of the pathway P in the relational equation.

The weighting index is composed of the product of three elements. We obtained the weighting index of all components using Eq. Among them, the weight index of the cumulative targets, ie, T_i , is determined by the weight index of the constituents because the YGG has multiple constituents that correspond to multiple targets. Finally, the targets are involved in the process of pathway functioning. Therefore, the weight index of each pathway was obtained and reordered based on the above relationships.

Network Construction and Functional Enrichment Analysis

The targets of YGG-regulated GA were identified, and we used Cytoscape 3.7 software to construct and visualize the “drug-compound-target” network. In addition, all targets regulating gouty arthritis were placed in the bioinformatics package and R software, and the genes were analyzed using GO functional enrichment analysis as well as KEGG pathway enrichment analysis. The results were reordered based on the weight index, and the critical value was set at $p < 0.05$.

Molecular Docking

The binding ability of the main components of YGG and the core protein was verified using a molecular docking technique. The PubChem database was used to obtain the component 3D structures, and the major protein receptor 3D structures were obtained from the UniProt database. Subsequently, PyMOL software was used to dehydrogenate the protein and remove the small molecule ligands from the protein receptor. Finally, the molecular docking of the treated protein receptors and ligands was performed using AutoDockTools 1.5.6 software, and their binding energies were recorded.

Transcriptomics Analysis

Using TRIzol reagent, total RNA was extracted from randomly selected synovial tissues. Determination of synovial tissue RNA concentration and integrity were performed using the Agilent 5400 Analyzer. The RNA purity was examined by agarose gel electrophoresis. Then, the obtained cDNA libraries were subjected to library quality control according, for

example, to the effective concentration. The HISAT2 software was used to align the measured genome with the reference genome. Based on the alignment results, Stringtie was used to reconstruct transcripts and RSEM was used to calculate the expression of all genes in each sample. Finally, we used DESeq2 software for differential expression analysis to obtain the differentially expressed genes of the samples. The Illumina NovaSeq 6000 was used to carry out the sequencing in its entirety. For more scientific sequencing results, differentially expressed genes were screened with a cutoff value of $p < 0.05$ and $|\text{Fold Change}| \geq 2$. GO and KEGG enrichment analyses were performed on differential genes using cluster Profiler software, and $p < 0.05$ was used as the threshold for screening significant enrichment results.

Immunohistochemical Analysis

The fixed tissues were washed using deionized water to remove impurities and then embedded using paraffin wax. Paraffin-embedded synovial tissue was dewaxed using xylene. Antigen repair was performed using citric acid antigen repair buffer and a microwave oven. Subsequently, the sections were incubated for 25 minutes at room temperature in 3% hydrogen peroxide to inhibit endogenous peroxidase. The primary antibody was applied overnight at 4 °C, and then the HRP-labeled secondary antibody was incubated for 60 min at room temperature. Finally, hematoxylin was used to restrain for 3 min, and images were acquired by microscopic photography.

Western Blot Analysis

Proteins were extracted from synovial tissue using RIPA tissue cell rapid lysate according to a standard protocol. BCA protein quantification reagent was used to determine the protein concentration in tissues. Then, according to the protein quantification results, the requisite proteins were added to the electrophoresis tank with the correct amount of loading buffer and PAGE gel, and an appropriate amount of electrophoresis buffer was added for electrophoretic separation and electrical transfer to a nitrocellulose membrane (NC). The membrane was blocked for 1 hour using 5% skim milk powder and incubated overnight at 4 °C with primary antibody. Finally, the HRP-labeled secondary antibody was incubated with the membrane for 1 h at 37 °C, and color development was performed by the Tanon-5200 system.

Statistical Analysis

Experimental data analyzed and mapped using IBM SPSS Statistics 26.0 and GraphPad Prism 8.3.0 softwares. Normally distributed data were tested using one-way ANOVA, data with a skewed distribution were tested using the Kruskal–Wallis test, and the post hoc test was performed using Tukey's test. A difference of $p < 0.05$ was considered statistically significant.

Results

YGG Chemical Composition Identification

The unknown analytes were identified by UPLC–ESI–MS/MS analysis, and positive and negative ion flow maps of all components of YGG were obtained (Figure 2). A total of 94 components were obtained, including apigenin, luteolin, rutin, paeonol, chuanxiong lactone A, paeoniflorin and ligustilide. Finally, the 94 components were attributed by the information of the herbal components included in TCMSP and reported in the literature, and the results are shown in [Table S1](#).

Effect of YGG on UA Generation in GA Progression

It is well known that elevated UA levels are the main manifestation of GA and are often used clinically along with Cr and BUN to assess kidney function status. In the model group, the kidney index was significantly increased ($p < 0.01$), indicating that elevated UA had a significant effect on the kidney (Figure 3A). UA levels in model group rats is significantly higher than the control group ($p < 0.01$), indicating the PO successfully induced rats of GA increased uric acid of symptoms (Figure 3B). However, both positive drug and different doses of YGG could effectively reverse this change, indicating that both drugs have therapeutic effects on UA elevation. Interestingly, the treatment effect in the YGG-H group was comparable to that of positive group. The effect of YGG on renal function was comprehensively

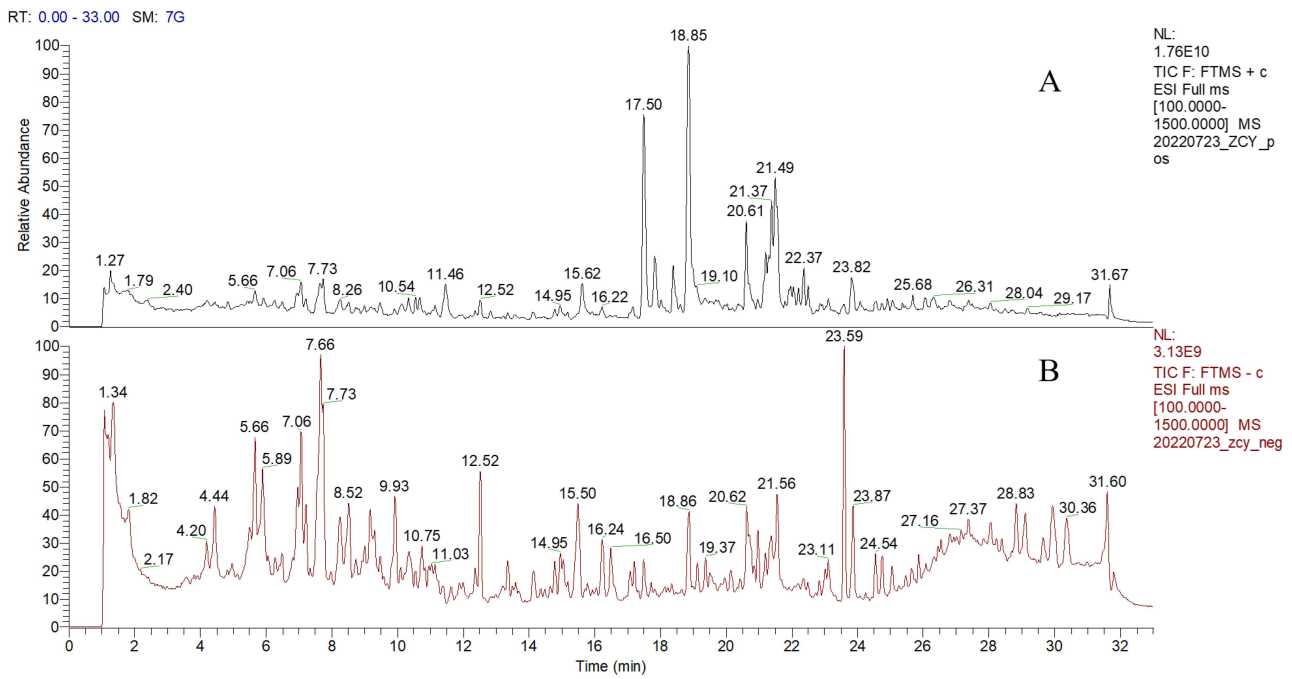


Figure 2 Total ion flow diagram in YGG positive (A) and negative (B) ion modes.

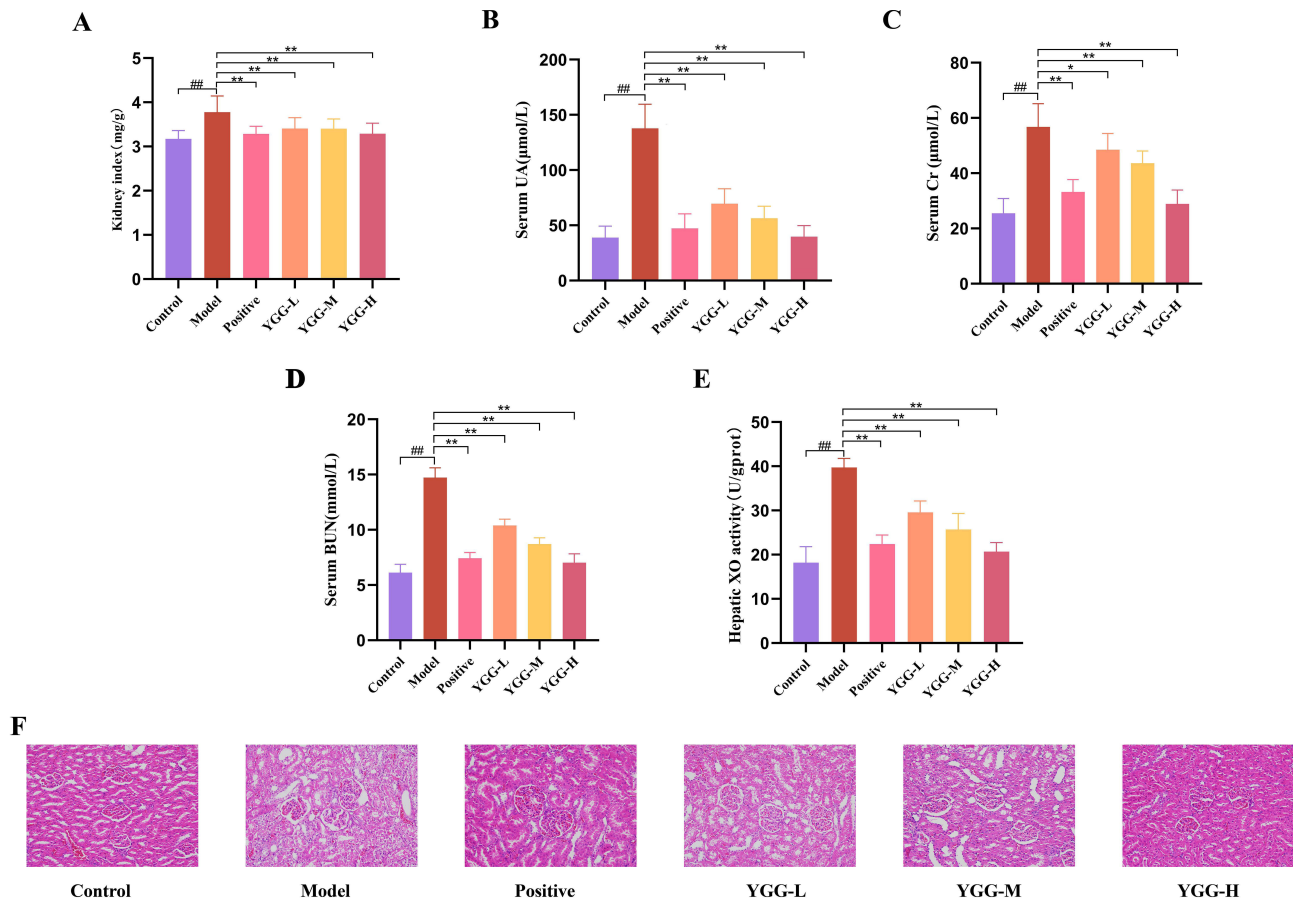


Figure 3 Effect of YGG on UA generation in GA progression. (A) Effect on kidney index. (B) Effect on UA in serum. (C) Effect on Cr in serum. (D) Effect on BUN in serum. (E) Effects on XO in liver tissue. Data are expressed as mean ± SD, (n=10), ##*p* < 0.01 compared with control group; **p* < 0.05, ***p* < 0.01 compared with model group. (F) Histological examination of the kidney with H & E staining (×200).

evaluated by measuring serum Cr and BUN. As shown in [Figure 3C–D](#), compared with the control group, the model group had noticeably elevated levels of serum Cr and UN ($p<0.01$), and after YGG treatment, serum Cr and BUN were significantly lower ($p<0.01$). The results showed that YGG was effective in suppressing the symptoms of UA elevation in GA. In addition, as shown in [Figure 3E](#), hepatic XO activity was significantly higher in the model group rats than in control rats ($p<0.01$). Hepatic XO activity was significantly downregulated after allopurinol treatment in the positive group rats. Similarly, hepatic XO activity was significantly decreased after YGG treatment ($p<0.01$). Details of the significance of the data are shown in [Table S2](#). The results suggest that YGG reduces UA production and accumulation in vivo by inhibiting hepatic XO activity. Kidney tissues HE dyed further confirmed the YGG can effectively reduce the UA level. The overall structure of normal rat kidney tissue was normal, with clear glomerular structure and no obvious degeneration, such as atrophy necrosis and dilated tubular pattern. The renal tubular epithelial cells did not show significant edema shedding necrosis, and the tissue was not infiltrated by obvious inflammatory cells. The kidney tissue results of the model group rats were abnormal, and a large amount of loose edema and necrotic detachment of renal tubular epithelial cells as well as marked dilatation were observed ([Figure 3F](#)).

Effect of YGG on the Inflammatory Response During GA Progression

Evaluation of ankle swelling in rats, as shown in [Figure 4A](#), revealed that the ankle joint swelling of rats in the model group was substantially greater than that of rats in the control group ($p<0.01$), while no significant changes were found in the ankle joint of the control group at any time after the injection of an equal volume of saline. This showed that intra-articular injections did not have any effect on the swelling of the ankle and that MSU-induced gouty arthritis modeling was a success. The degree of swelling in the rats reached its peak 12 h after modeling, when redness and swelling were evident in the right joint. Notably, the model group showed greater joint swelling than the control group at different time points.

We measured the serum levels of IL-1 β , IL-6, and TNF- α in rats to assess the anti-inflammatory effects of YGG ([Figure 4B–D](#)). The model group levels of IL-1 β , IL-6, and TNF- α were significantly higher than those of the control group ($p<0.01$), suggesting that MSU-induced gouty arthritis was accompanied by an acute inflammatory response. YGG significantly reduced the production of IL-1 β , IL-6 and TNF- α in serum ($p<0.01$) compared with the model group. In addition, the effects of MSU-induced inflammation were further evaluated by measuring the levels of COX-2, PGE2, IL-1 β , IL-6 and TNF- α in synovial tissue ([Figure 4E–I](#)). The levels of COX-2, PGE2, IL-1 β , IL-6 and TNF- α were significantly increased in the MSU-induced model group compared to the control group ($p<0.01$), and the production of COX-2, PGE2, IL-1 β , IL-6 and TNF- α in synovial tissue was shown to be considerably reduced in the YGG therapy group ($p<0.01$). Details of the significance of the data are shown in [Table S3](#).

HE staining further verified the above assay results. The synovial tissue of rats in the model group showed more synovial cells with obvious necrosis, nuclear consolidation and lysis of synovial cells, and severe inflammatory cell infiltration. After YGG treatment, the synovial structure of the tissue was clear, and the aforementioned pathological modifications improved significantly ([Figure 4J](#)). Based on the data, YGG improved the degeneration of synovial cells, as evidenced by sparing, edema, proliferation, and necrosis, inhibited inflammatory cell infiltration and had significant therapeutic effects on MSU-induced inflammation.

Network Pharmacology Analysis

YGG Component Screening

Using $OB \geq 30\%$ and $DL \geq 0.18$ as the screening criteria, the 94 identified major components were further screened. Due to the incompleteness of the database, all components could not be fully considered. Therefore, on the basis of database screening, components clearly reported to have medicinal value in the literature were also included in the active components of YGG to achieve a comprehensive study. The final 42 active components were obtained ([Table 3](#)), and these active components were used as the basis for network pharmacology prediction.

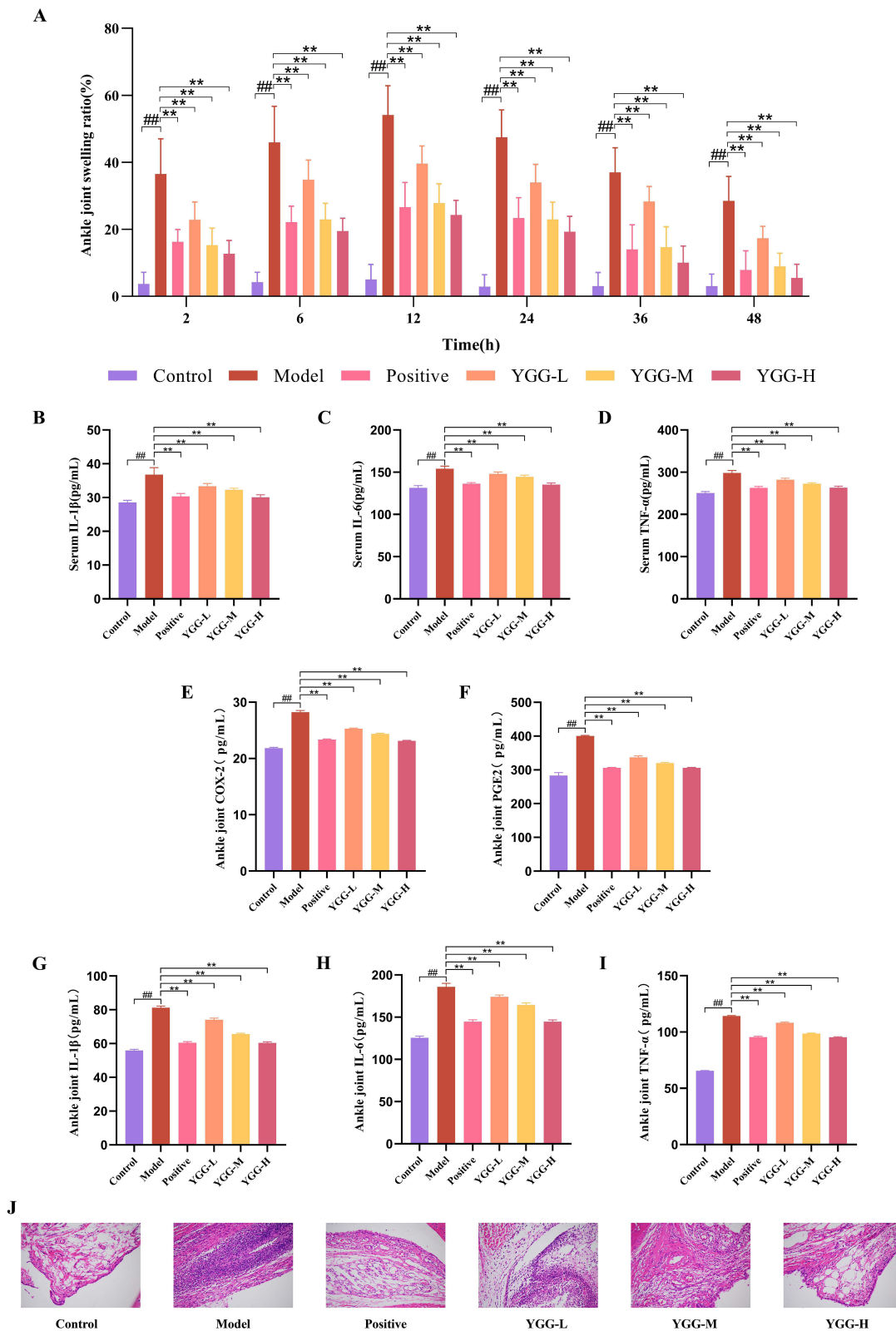


Figure 4 Effect of YGG on the inflammatory response during GA progression. **(A)** Determination of right ankle joint swelling in rats at different time points (2, 6, 12, 24, 36, 48 h) after MSU suspension injection. **(B–D)** Effects on serum IL-1β, IL-6 and TNF-α. **(E)** Effect on COX-2 in ankle joint. **(F)** Effect on PGE2 in ankle joint. **(G–I)** Effects on IL-1β, IL-6 and TNF-α in ankle joint. Data are expressed as mean ± SD, (n=10), ###*p* <0.01 compared with control group; ***p* <0.01 compared with model group. **(J)** Histological examination of the synovial with H & E staining (×200).

Table 3 Main Active Ingredient of YGG

MOL ID	Name	OB%	DL	Herb
MOL001955	Chlorogenic acid	11.93%	0.33	Lonicera japonica Flos
MOL003065	Cryptochlorogenic acid	10.48%	0.33	Lonicera japonica Flos
MOL000008	Apigenin	23.06%	0.21	Lonicera japonica Flos
MOL000006	Luteolin	36.16%	0.25	Lonicera japonica Flos
MOL002881	Diosmetin	31.14%	0.27	Lonicera japonica Flos
MOL000009	Cynaroside	7.29%	0.78	Lonicera japonica Flos
MOL003118	Isochlorogenic acid C	1.78%	0.69	Lonicera japonica Flos
MOL003067	Isochlorogenic acid B	1.71%	0.69	Lonicera japonica Flos
MOL001875	Isochlorogenic acid A	1.79%	0.69	Lonicera japonica Flos
MOL000432	α -Linolenic acid	45.01%	0.15	Scrophulariae Radix
MOL007088	Cryptotanshinone	52.34%	0.4	Scrophulariae Radix
MOL000737	Morin	0.4623	0.27	Rehmanniae Radix
MOL009289	Calycosin-7-O- β -D-glucoside	41.60%	0.81	Glycyrrhizae Radix Et Rhizoma
MOL004876	Glycyrrhizic acid	19.62%	0.11	Glycyrrhizae Radix Et Rhizoma
MOL004804	18 β -Glycyrrhetintic Acid	22.05%	0.74	Glycyrrhizae Radix Et Rhizoma
MOL001789	Isoliquiritigenin	85.32%	0.15	Glycyrrhizae Radix Et Rhizoma
MOL000417	Calycosin	47.75%	0.24	Glycyrrhizae Radix Et Rhizoma
MOL002928	Oroxylin A	41.37%	0.23	Glycyrrhizae Radix Et Rhizoma
MOL004841	Licochalcone B	76.76%	0.19	Glycyrrhizae Radix Et Rhizoma
MOL004912	Glabrone	52.51%	0.5	Glycyrrhizae Radix Et Rhizoma
MOL000497	Licochalcone A	40.79%	0.29	Glycyrrhizae Radix Et Rhizoma
MOL004903	Liquiritin	65.59%	0.74	Glycyrrhizae Radix Et Rhizoma
MOL000874	Paeonol	28.79%	0.04	Paeoniae Radix Alba
MOL001924	Paeoniflorin	53.87%	0.79	Paeoniae Radix Alba
MOL007003	Benzoylpaeoniflorin	31.27%	0.75	Paeoniae Radix Alba
MOL000044	Atractylenolide II	47.50%	0.15	Atractylodis macrocephala Rhizoma
MOL000045	Atractylenolide III	68.11%	0.17	Atractylodis macrocephala Rhizoma
MOL002208	Senkyunolide A	26.56%	0.07	Chuanxiong Rhizoma
MOL002124	α -Asarone	35.61%	0.06	Chuanxiong Rhizoma
MOL002189	3-n-Butylphthalide	47.90%	0.07	Angelicae sinensis Radix
MOL002111	3-Butylidenephthalide	42.44%	0.07	Angelicae sinensis Radix
MOL000701	Quercitrin	4.04%	0.74	Amomi Fructus
MOL000437	Isoquercitrin	1.86%	0.77	Amomi Fructus
MOL000414	Caffeic acid	54.97%	0.05	Lonicera japonica Flos, Scrophulariae Radix
MOL003333	Verbascoside	2.94%	0.62	Scrophulariae Radix, Rehmanniae Radix
MOL000360	FER	39.56%	0.06	Scrophulariae Radix, Angelicae sinensis Radix, Rehmanniae Radix, Chuanxiong Rhizoma
MOL000748	5-Hydroxymethylfurfural	45.07%	0.02	Scrophulariae Radix, Rehmanniae Radix, Amomi Fructus
MOL002201	Ligustilide	51.30%	0.07	Angelicae sinensis Radix, Chuanxiong Rhizoma
MOL002102	Levistilide A	2.15%	0.82	Angelicae sinensis Radix, Chuanxiong Rhizoma
MOL000415	Rutin	3.20%	0.68	Lonicera japonica Flos, Glycyrrhizae Radix Et Rhizoma
MOL000561	Astragaln	14.03%	0.74	Lonicera japonica Flos, Glycyrrhizae Radix Et Rhizoma, Paeoniae Radix Alba, Dioscoreae Rhizoma
MOL000513	Gallic acid	31.69%	0.04	Paeoniae Radix Alba, Chuanxiong Rhizoma

Potential Targets of YGG in the Treatment of GA

The results are shown in [Figure 5A](#). Venn diagrams were constructed by matching the drug component targets with the disease gene targets. A total of 908 disease targets and 666 component targets were identified, with 223 targets being

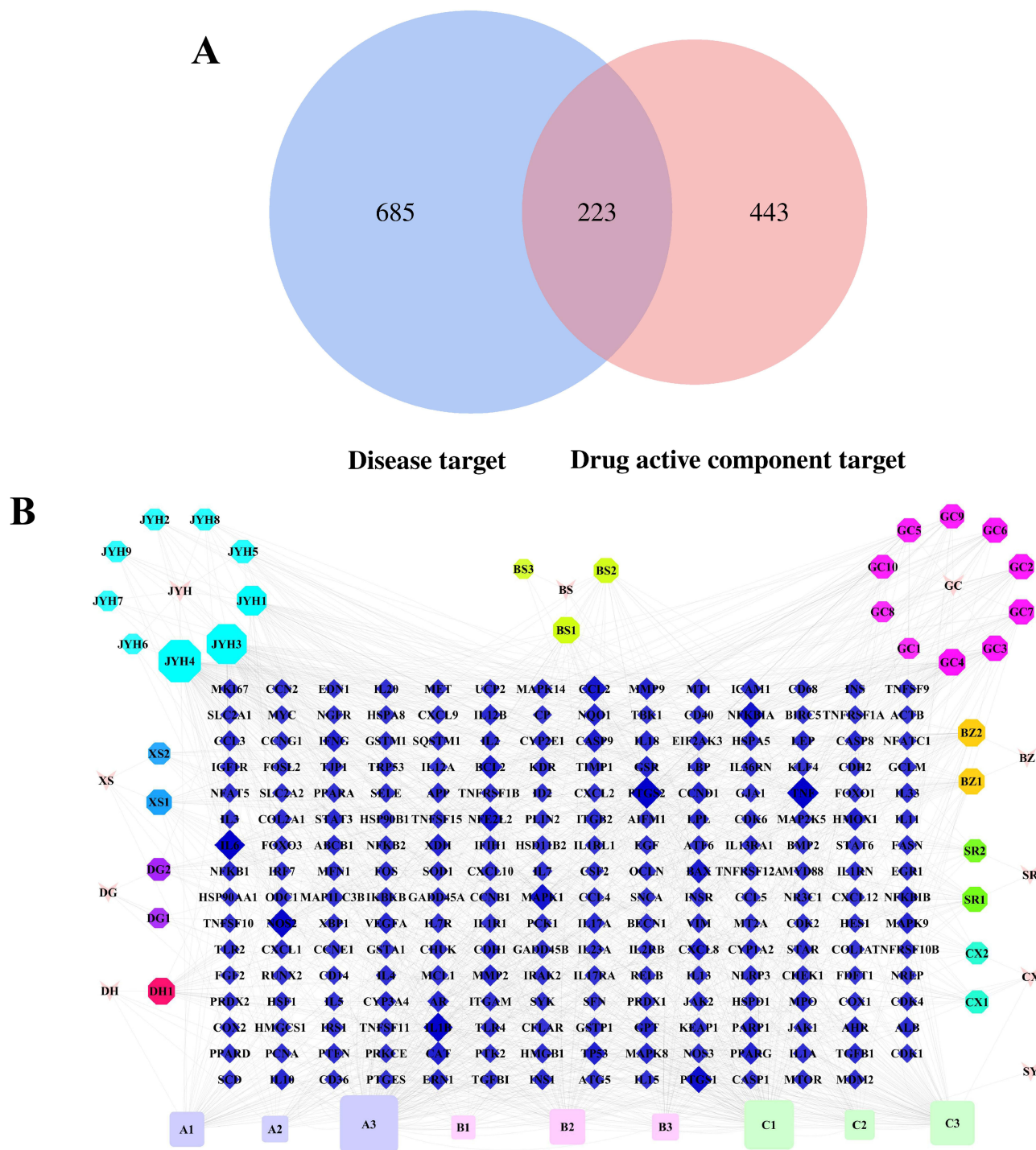


Figure 5 Network pharmacology predicts potential targets of YGG for GA treatment. **(A)** Venn diagram of YGG component genes and GA genes. **(B)** YGG drug-component-target network diagram. The following is a detailed annotation of the common components of the different herbs of YGG. A1: Caffeic acid, A2: Verbascoside, A3: Ferulic acid, B1: 5-Hydroxymethylfurfural, B2: Ligustilide, B3: Levistilide A, C1: Rutin, C2: Astragalin, C3: Gallic acid.

found to be common between drug components and diseases. The results suggest that the drug components corresponding to these intersecting targets may have therapeutic effects on GA.

Construction of the Drug-Component-Target Interaction Network

The drug-component-target network includes a total of 275 nodes and 1392 edges (Figure 5B). The triangle indicates the drug, the circle indicates the component, the square indicates the shared component, and the diamond indicates the gene

target. The degree of a node reflects the number and strength of links connected to the node and is a measure of the degree to which the node is embedded in the network. The larger the degree value, the more connected the nodes, and the more important the corresponding drug components.

Establishment of the YGG Weighting Index

Based on the pharmacological effects of the monarchs and minister of YGG and the components reported in the literature, we used 10 herbs as indicators for the weighting index and determined the priority of each indicator as follows: *Lonicera japonica* Flos > *Scrophulariae Radix* = *Angelicae sinensis Radix* > *Rehmanniae Radix* = *Paeoniae Radix Alba* = *Chuanxiong Rhizoma* = *Glycyrrhizae Radix Et Rhizoma* > *Atractylodis macrocephala Rhizoma* = *Amomi Fructus* = *Dioscoreae Rhizoma*. The weighting indices of the herbs are shown in Table 4. The weight indices of the 10 herbs calculated using the AHP method were 15.676% for *Lonicera japonica* Flos, 12.538% for *Scrophulariae Radix* and *Angelicae sinensis Radix*, 9.517% for *Rehmanniae Radix*, *Paeoniae Radix Alba*, *Chuanxiong Rhizoma* and *Glycyrrhizae Radix Et Rhizoma*, and 7.059% for *Atractylodis macrocephala Rhizoma*, *Amomi Fructus* and *Dioscoreae Rhizoma*.

GO Functional Enrichment and KEGG Pathway Enrichment Analyses

To elucidate the biological functions of the 223 targets and identify their associated key pathways, GO and KEGG enrichment analyses were conducted. A total of 2730 biological processes (BP), 174 molecular functions (MF), 55 cellular components (CC) and 148 KEGG pathways were obtained. The obtained enrichment items were reordered, and the results are shown in Figure 6.

GO enrichment analysis before screening: The targets were mainly distributed in cellular components such as membrane rafts, membrane microdomains, endoplasmic reticulum lumen, organelle outer membrane, and plasma membrane signaling receptor complexes. The targets are involved in biological processes such as cellular responses to biological stimuli and lipopolysaccharides through cytokine activity and phosphatase binding. After rescreening by weighting index, the targets are mainly distributed in cellular fractions such as plasma membrane rafts and cytoplasmic vesicle lumen. Through cytokine receptor binding, cytokine and receptor ligand activity, and other mechanisms, it participates in the positive regulation of cytokine production, the inflammatory response, leukocyte-mediated immunity, and other biological processes.

KEGG pathway enrichment analysis prior to screening: The targets are mainly involved in signaling pathways such as cytokine–cytokine receptor interactions, PI3K-Akt and MAPK. After rescreening by weighting index, signaling pathways such as NF- κ B, TNF and IL-17, in which the targets are involved, are more closely related to gouty arthritis.

YGG Main Active Components

The top 10 active components with degree values obtained by Cytoscape 3.7.1 software were ferulic acid, rutin, gallic acid, luteolin, apigenin, ligustilide, caffeic acid, astragalol, chlorogenic acid and paeonol. Combined with literature reports, these components were finally identified as the main active components of YGG, as shown in Table 5. The top 6

Table 4 YGG Drug Weighting Index

Ingredient	Eigenvector	Weighting Value (%)	Maximum Characteristic Root	CI
<i>Lonicera japonica</i> Flos	1.622	15.676	10.019	0.002
<i>Scrophulariae Radix</i>	1.297	12.538		
<i>Angelicae sinensis Radix</i>	1.297	12.538		
<i>Rehmanniae Radix</i>	0.985	9.517		
<i>Paeoniae Radix Alba</i>	0.985	9.517		
<i>Chuanxiong Rhizoma</i>	0.985	9.517		
<i>Glycyrrhizae Radix Et Rhizoma</i>	0.985	9.517		
<i>Amomi Fructus</i>	0.730	7.059		
<i>Atractylodis macrocephala Rhizoma</i>	0.730	7.059		
<i>Dioscoreae Rhizoma</i>	0.730	7.059		

Table 6 YGG Main Active Target Information Table

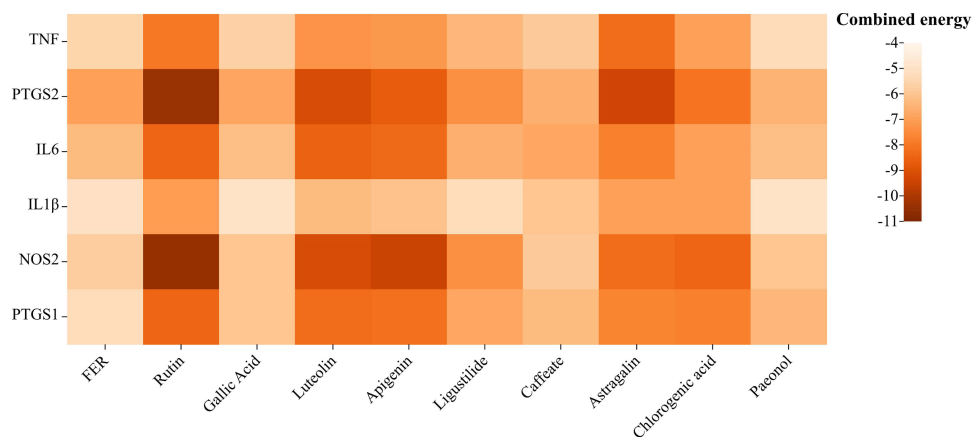
Active Target	Degree
TNF	52
PTGS2	51
IL6	47
IL1B	42
NOS2	40
PTGS1	33

Table 7 Docking Binding Energy of the Main Active Ingredients of YGG to the Target Protein Molecules (Kcal/Mol)

	FER	Rutin	Gallic Acid	Luteolin	Apigenin	Ligustilide	Caffeic Acid	Astragaln	Chlorogenic Acid	Paeonol
TNF	-5.5	-8	-5.7	-7.3	-7.2	-6.4	-5.9	-8.3	-7	-5.3
PTGS2	-7	-10.4	-6.9	-9.2	-8.7	-7.4	-6.6	-9.4	-8.1	-6.5
IL6	-6.3	-8.5	-6.2	-8.6	-8.4	-6.6	-6.8	-7.8	-7	-6.2
IL1B	-5.1	-7.1	-5	-6.3	-6.1	-5.2	-6	-7	-7	-5
NOS2	-5.8	-10.5	-6	-9.2	-9.5	-7.4	-5.9	-8.3	-8.5	-6
PTGS1	-5.2	-8.5	-6	-8.3	-8.2	-6.8	-6.3	-7.7	-7.8	-6.4

transcriptomics. Analysis of biochemical indices, expression levels of inflammatory factors and pathological sections in animal experiments showed that the YGG-H group was effective in the treatment of gouty arthritis. Moreover, the inhibitory effect was significantly higher than that of YGG-L and YGG-M. Therefore, the YGG-H group was selected as the treatment group for transcriptomic analysis.

Between the control and model groups, a total of 424 differentially expressed genes (DEGs) were found, 227 of which were upregulated and 197 of which were downregulated (Figure 8A). In the model and YGG-H groups, a total of 1158 DEGs were identified, of which 767 were upregulated and 391 were downregulated (Figure 8B). A total of 1604 DEGs were identified in the control group and YGG-H group, of which 1128 were upregulated and 476 were downregulated (Figure 8C). Cluster analysis visually showed (Figure 8A–C) that the expression levels of DEGs changed significantly between groups, and the upregulated DEGs caused by MSU were significantly reversed after YGG treatment. These results suggest that large changes in rat synovial tissue genes occur after MSU injection, and early feeding of YGG can inhibit this change to some extent, which is consistent with the biochemical index findings.

**Figure 7** Docking binding energy information of YGG active component and core target molecules.

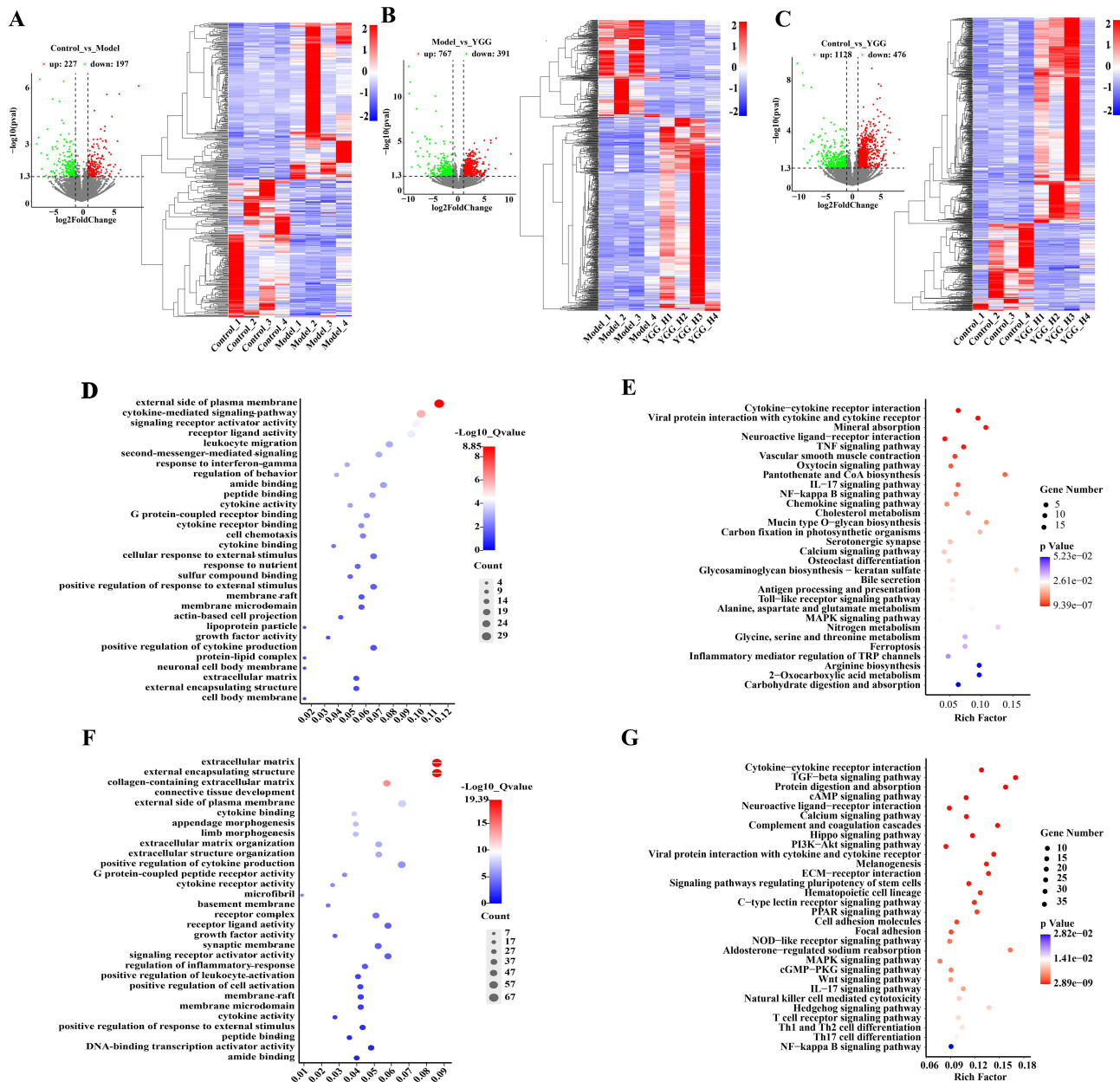


Figure 8 Transcriptomic analysis reveals the signaling pathway of YGG treatment of GA. **(A)** Volcano plot showing the number of DEGs in the control group vs the model group; and these DEG heatmaps. Blue indicates downregulated genes and red indicates upregulated genes. **(B)** Volcano plot showing the number of DEGs in the model group vs the YGG group; and heat map of these DEGs. Blue indicates downregulated genes and red indicates upregulated genes. **(C)** Volcano plot showing the number of DEGs in the control group vs the YGG group; and a heat map of these DEGs. Blue indicates downregulated genes and red indicates upregulated genes. **(D-E)** GO enrichment in the top 30 DEG rankings in the control group vs in the model group; KEGG enrichment in the top 30 DEG rankings. **(F-G)** GO enrichment in the top 30 DEG rankings in the model group vs in the YGG group; KEGG enrichment in the top 30 DEG rankings.

In addition, further transcriptomics-based enrichment analysis was performed to reveal the underlying mechanism of this change. Analysis of GO enrichment of DEGs in the control and model groups revealed (Figure 8D) that DEGs are predominantly distributed in membrane rafts, plasma membrane rafts, extracellular matrix, and lipoprotein particles. The targets are involved in biological processes such as leukocyte migration, cytokine-mediated signaling pathways, positive regulation of cytokine production, and cellular response to external stimuli through signaling receptor activator activity, peptide binding activity, and protein-coupled receptor binding. Expression of the GO enrichment analysis of DEGs in the model and YGG groups (Figure 8F). DEGs are mainly distributed in cellular components such as membrane microdomains, the extracellular matrix, synaptic membranes, and receptor complexes. The targets are implicated in the

regulation of the inflammatory response and other biological processes through cytokine binding, DNA-binding transcriptional activator activity, and cytokine receptor activity. Taken together, YGG may treat gouty arthritis through inflammatory response modulation, which remains consistent with the pathological section results. KEGG pathway analysis was used to assess the biological significance of YGG for GA and to elucidate the multipathway multitarget effects of YGG for MSU-mediated GA. KEGG enrichment analysis of DEGs in the control and model groups (Figure 8E) showed that a total of 178 pathways were enriched, among which the TNF, NF- κ B, IL-17 and MAPK signaling pathways were the most significant. KEGG enrichment analysis of DEGs in the model and YGG groups (Figure 8G) showed that a total of 200 pathways were enriched, among which the PI3K-Akt, NF- κ B, and IL-17 signaling pathways were the most significant. In summary, MSU may alter the expression levels of DEGs through the IL-17 and NF- κ B signaling pathways to cause gouty arthritis, while YGG reverses this change by regulating the NF- κ B, IL-17, and MAPK signaling pathways, which in turn inhibits inflammation.

YGG Suppresses Inflammation Through Regulation of the TLR4/MYD88/NF- κ B Signaling Pathway

Network pharmacological predictions at the theoretical level revealed that the NF- κ B, TNF and IL-17 signaling pathways were more closely related to gouty arthritis, whereas transcriptomic assays at the practical level revealed that the NF- κ B, IL-17, and MAPK signaling pathways were significantly enriched in the synovial tissues of GA rats after administration of high doses of YGG. Animal experiments showed that YGG inhibited the expression of inflammatory factors in serum and synovial tissues of GA rats, further confirming that this potential mechanism of action is inextricably linked to the regulation of Inflammatory response. Combined with the above experimental results, we believe that YGG achieves inhibition of the GA process through the NF- κ B signaling pathway. In addition, NF- κ B is readily recognized by TLR4 and MYD88, allowing increased expression of downstream inflammatory proteins such as IL-1 β and TNF- α , which in turn cause an inflammatory response.^{20,21} Therefore, we believe that the TLR4/MYD88/NF- κ B signaling pathway may be YGG inhibition of GA in precise mechanism, and in the following experiment to validate it.

IHC was used to confirm the effect of YGG on the dysregulated TLR4/MYD88/NF- κ B signaling pathway (Figure 9). Details of the significance of the data are shown in Table S4. Key proteins of the pathway, including TLR4, MYD88, p65, p-p65, IKK α/β , p-IKK α/β , I κ B α , and p-I κ B α , were identified using Western blot. In contrast to the model group, TLR4 and MYD88 expression levels and the p65/p-p65, IKK α/β /p-IKK α/β , and I κ B α /p-I κ B α ratios in the synovial tissue of rats in the YGG group were significantly reduced in a dose-dependent manner (Figure 10). Details of the significance of the data are shown in Table S5. The results suggested that YGG treated the impaired TLR4/MyD88/NF- κ B signaling pathway.

Discussion

Chinese medicine is effective in treating gout. Compared with conventional Western medical treatment, Chinese medicine treatment has the characteristics of multiple components, multiple pathways, and both primary and secondary treatment, and the compound prescription of Chinese medicine follows the principle of the combination of monarchs and minister. From a holistic perspective, the systemic regulation of the organism is achieved through the active components of the drug.²² Despite years of research into the treatment of GA and some proof of the scientific validity of the research, the number of people with GA continues to increase.^{23–26} The possible causes of this phenomenon are as follows: (i) insufficient attention is given to the prevention of the chronic disease HUA, leading to the deterioration of the disease and its development from HUA to GA; and (ii) the pathogenesis of GA is closely related to diet and lifestyle. Unfortunately, most people have a hard time maintaining a healthy lifestyle. (iii) As we age, the organism becomes susceptible to chronic diseases. YGG has been clinically proven to be effective and safe as an anti-inflammatory therapy for GA.²⁷

HUA, as an important pathological basis of GA, is closely related to GA. In this study, potassium oxonate combined with MSU was used to establish a rat model of GA, which can well simulate the development of GA in clinical patients. That is, from the initial elevated levels of UA in the body, to the gradual deposition of MSU in the joints resulting in an inflammatory response that eventually develops into GA.²⁸ XO is a crucial enzyme in the development of gout and is

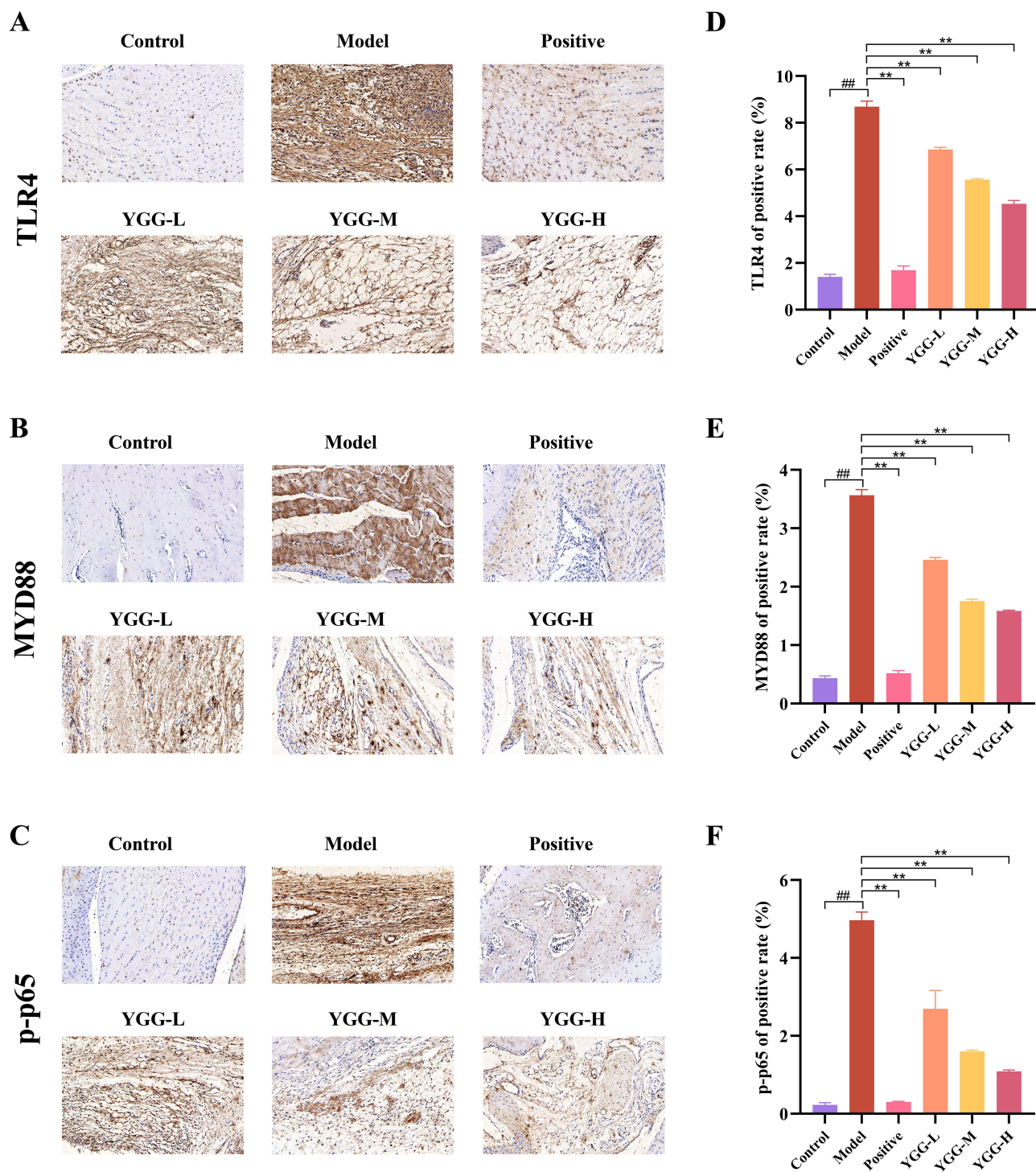


Figure 9 TLR4, MYD88, p-p65 IHC stains in rat synovial tissue. (A–C) IHC shows the expression of TLR4, MYD88 and p-p65 in rat synovial tissue (Scale bar: 50µm). (D–F) Quantification of TLR4, MYD88 and p-p65 in rat synovial tissue. Data are expressed as mean ± SD, (n=6), ###p <0.01 compared with control group; **p <0.01 compared with model group.

involved in the process of excessive UA production.²⁹ Therefore, measuring XO activity is important to explain the mechanism of action of how YGG reduces UA levels. We found that after oral administration of YGG, the treatment group significantly inhibited liver XO activity, thereby significantly reducing UA levels. In addition, Cr and BUN are two important indicators of renal function, and Cr and BUN have been shown to correlate with glomerular filtration rate and

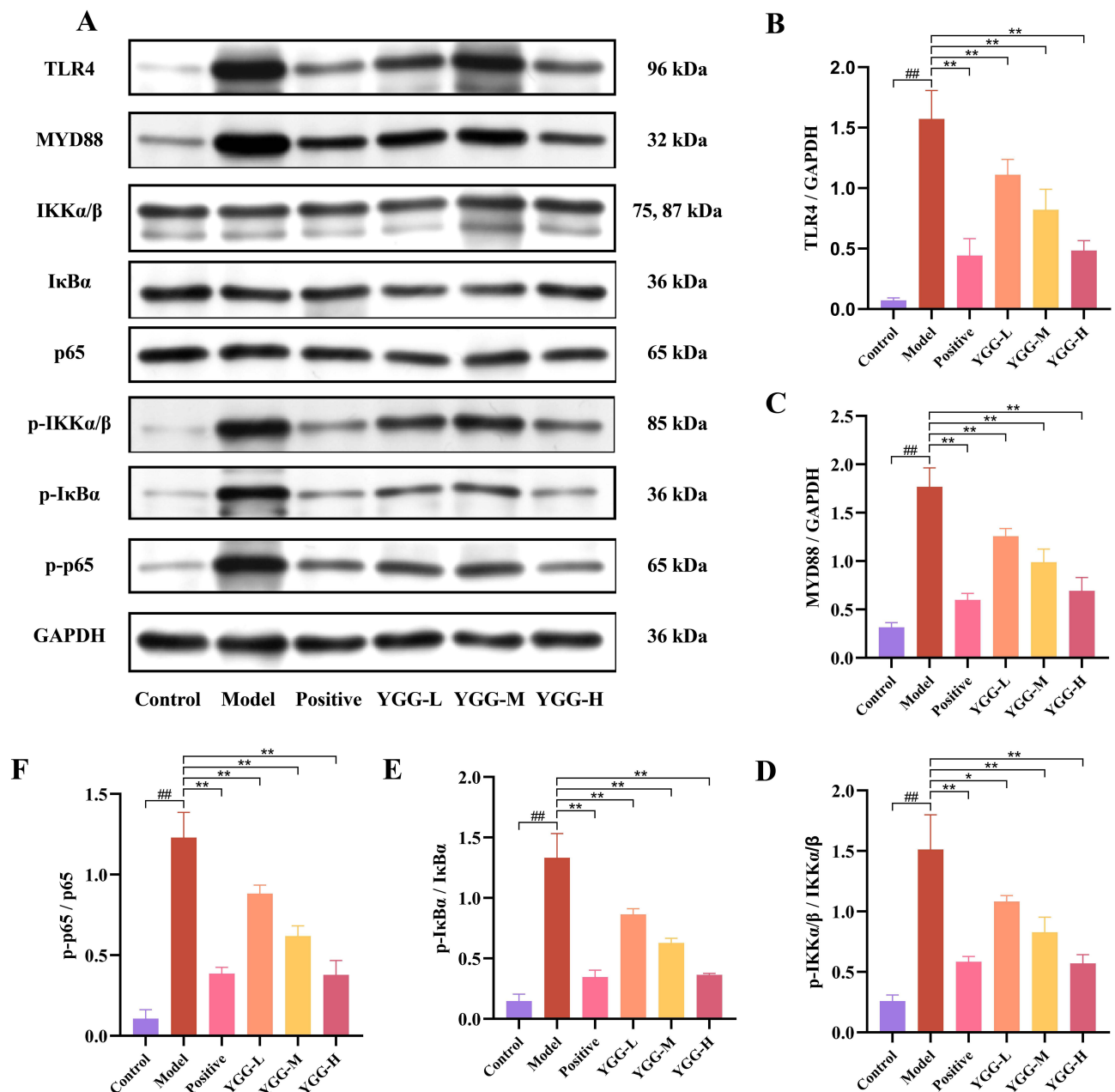


Figure 10 YGG suppresses inflammatory responses by regulating TLR4/MYD88/NF- κ B signaling pathway. **(A)** The expression of TLR4, MYD88, p65, p-p65, IKK α/β , p-IKK α/β , I κ B α and p-I κ B α by Western blot. **(B–F)** Quantitative analysis of Western blot for TLR4, MYD88, p-IKK α/β /IKK α/β , p-I κ B α /I κ B α , p-p65/p65. Data are expressed as mean \pm SD, (n=3), ### p <0.01 compared with control group; * p <0.05, ** p <0.01 compared with model group.

kidney function.³⁰ The results showed that all groups of YGG significantly reduced the expression levels of serum Cr and UN in rats compared with the model group. This finding was confirmed in histopathological studies of the kidney. In addition, the key to treating GA is to suppress inflammation. IL-1 β is a highly inflammatory factor that is closely associated with GA.³¹ IL-6 acts as an inflammatory stimulator and induces the synthesis of reactive proteins in the inflammatory response,³² which in turn exacerbates the GA inflammatory response. TNF- α is a factor that contributes to inflammation and plays a significant role in both acute and chronic forms of the condition.³³ The primary function of COX-2 is to accelerate the transformation of arachidonic acid into the neurotoxic metabolite PGE2, which in turn encourages the release of inflammatory mediators and the progression of neurodegenerative disorders.^{34,35} The results of this experiment showed that YGG could inhibit the expression of IL-1 β , IL-6, and TNF- α proinflammatory factors as

well as COX-2 and PGE2 in the serum and synovial tissues of GA rats induced by MSU. The same histopathological examination of the rat synovial membrane demonstrated that YGG could significantly inhibit the development of inflammation. In conclusion, YGG is clearly useful in the treatment of GA.

The analysis was performed by UPLC-ESI-MS/MS, and the online mzCloud spectral library and Thermo Scientific mzVault spectral library were searched using Compound Discoverer 3.0 software. 94 major components of YGG were identified. Then, 94 components were attributed by TCMSP and literature studies. There were 24 kinds of *Lonicera japonica* Flos, 8 kinds of *Scrophulariae Radix*, 11 kinds of *Angelicae sinensis Radix*, *Rehmanniae Radix* and *Chuanxiong Rhizoma*, 23 kinds of *Glycyrrhizae Radix ET Rhizoma*, 10 kinds of *Paeoniae Radix Alba*, 7 kinds of *Amomi Fructus*, 2 kinds of *Dioscoreae Rhizoma* and 2 kinds of *macrocephala Rhizoma*. However, for the attribution of major components, nine components were found to be not attributed to the herbs in the compounds, probably due to false-positives when matching drug components using the database, which can be subsequently confirmed by standard calibration. Network pharmacology is frequently employed to investigate the mechanism of action of herbal medications because it facilitates the analysis of the connection between different components, relevant targets and diseases of herbal medicines.³⁶ Therefore, in this experiment, 45 active components of YGG were screened from 94 main components by a network pharmacological study. We also predicted the 10 active components and core targets of YGG for the treatment of gouty arthritis by Cytoscape software with degree as the criterion. Combined with molecular docking techniques to determine the binding ability of the active components to the core targets, the active components of YGG for GA were further validated. In this experiment, 10 main active components in YGG were screened and obtained, namely, ferulic acid, rutin, gallic acid, luteolin, apigenin, ligustilide, caffeic acid, astragaloside, chlorogenic acid and paeonol, and all of them demonstrated anti-inflammatory properties. Among them, paeonol can inhibit inflammation by decreasing the levels of TNF- α and IL-6 and increasing the expression of IL-10. Ferulic acid inhibits the NF- κ B inflammatory pathway and reduces IL-1 β and TNF- α expression under mild oxidative stress.³⁷ Rutin effectively ameliorates the inflammatory response by reducing the proinflammatory factor markers IL-1 β , TNF- α , IL-6 and COX-2 through its powerful antioxidant characteristics.³⁸ Gallic acid blocks NLRP3 inflammasome activation, caspase-1 activation, and IL-1 β production in mice to reduce GA effects.³⁹ Apigenin has antioxidant, anti-inflammatory and XO activity-inhibiting effects.⁴⁰ Ligustilide is able to reduce inflammation by inhibiting the TLR4/NF- κ B signaling pathway and suppressing P38/MAPK phosphorylation activation. Caffeic acid can reduce the expression of NF- κ B, IL-1 β and Caspase-3, thus exerting anti-inflammatory effects.⁴¹ Astragaloside plays an important pharmacological role in the inflammatory response and oxidative stress, which significantly inhibits the release of inflammatory factors and reduces apoptosis.⁴² Chlorogenic acid, one of the abundant polyphenols in Chinese medicine, can improve MSU crystal-induced inflammatory symptoms by inhibiting the production of IL-1 β , IL-6 and TNF- α .⁴³ It is clear from the information presented above that the principal active components are able to control the inflammatory response and produce the desired effect of GA treatment by modulating the expression of key targets.

However, the database on which network pharmacology is based has limitations and lags, resulting in a failure to reflect the true network characteristics within the organism in a timely manner. Second, the influence of the content of herbal components is often ignored during pharmacological studies of traditional Chinese medicine networks, resulting in a lack of reliability of the potential mechanisms of action obtained. Therefore, we sought to disclose the pharmacological mechanism of YGG for GA with greater precision. First, the weighted method was used to obtain a more comprehensive screening of the results of GO and KEGG enrichment analysis obtained from traditional network pharmacology in terms of the dispensing pattern of YGG and the oral bioavailability of drug components. Among them, the drug pathways of action changed significantly according to the weighting index. For example, the NF- κ B inflammatory pathway (from the 24th to 11th days after screening) and the IL-17 signaling pathway (from the 19th to 6th days after screening). The results suggest that with the addition of the weighting index, network pharmacology predicts a more plausible mechanism of action. Afterward, we performed an integrated network pharmacology and transcriptomics analysis, which finally confirmed that YGG inhibits the development of inflammation by regulating the TLR4/MYD88/NF- κ B signaling pathway.

In the development of inflammation, the production of various inflammatory cytokines is attributed to the activation of TLR4 signaling, and its activation activates MYD88. MYD88 acts as a downstream protein of TLR4 and is required for the induction of translocation of the transcription factor NF- κ B to the nucleus.⁴⁴ NF- κ B, a group of inflammation-associated

transcription factors, consists mainly of heterodimers of p65 and p50 and can bind to I κ B α . It is worth noting that p65 isomer is usually considered a NF - κ B complex main activation of transcription factors, and has important effect on the activation of the inflammatory response. A large number of studies have shown that the p65 isoforms involved in NF- κ B in the TLR4/MYD88/NF- κ B pathway are more prevalent and intensively investigated, suggesting that the p65 isoforms may play a more important role in the TLR4/MYD88/NF- κ B pathway.^{45,46} Under normal conditions, NF- κ B is tightly bound to I κ B α in the cytoplasm. Activated IKK α / β catalyzes the phosphorylation and degradation of I κ B α when stimulated by some inflammatory substances. Subsequently, NF- κ B is released and activated, at which point NF- κ B is also phosphorylated in the nucleus to promote gene expression.⁴⁷⁻⁵¹ This may further help stimulate the expression of downstream proteins such as COX-2 and IL-1 β and ultimately contribute to the inflammatory response.⁵²⁻⁵⁴ We validated this process in the IHC study. We observed that the expression levels of TLR4, MYD88, and p-p65 were significantly elevated in the model group, and following YGG therapy, the expression of these proteins was decreased. Western blot was used to analyze the proteins involved in this pathway to further elucidate how the pathway is altered during inflammation. We found that the expression of TLR4, MYD88, p-p65, p-IKK α - β , and p-I κ B α was significantly increased in the model group compared with the YGG group. Our joint analysis jointly confirmed, in terms of both theoretical predictions and practical findings, that YGG suppresses the inflammatory development of GA by regulating the TLR4/MYD88/NF- κ B signaling pathway (Figure 11).

This research study and the combination of network pharmacology by transcriptome analysis, from the theoretical level to practical level, for the treatment of YGG GA accurate way to make the complete description and validation. For the complex mechanisms of traditional Chinese medicine research, it is good. At the same time, the good anti-GA effect of YGG also provides a reliable candidate drug for clinical application, and improves the limitation of drug use in GA patients. However, these studies have certain limitations. Although p65 subtypes in TLR4/MYD88/NF- κ B signal pathway plays a more vital role, but the further research must also be considered p50 or p65 + p50 combination in the role of GA. It can extend the scope of the current study, can also for further understanding of the role of NF - κ B in inflammatory response provide a new perspective.

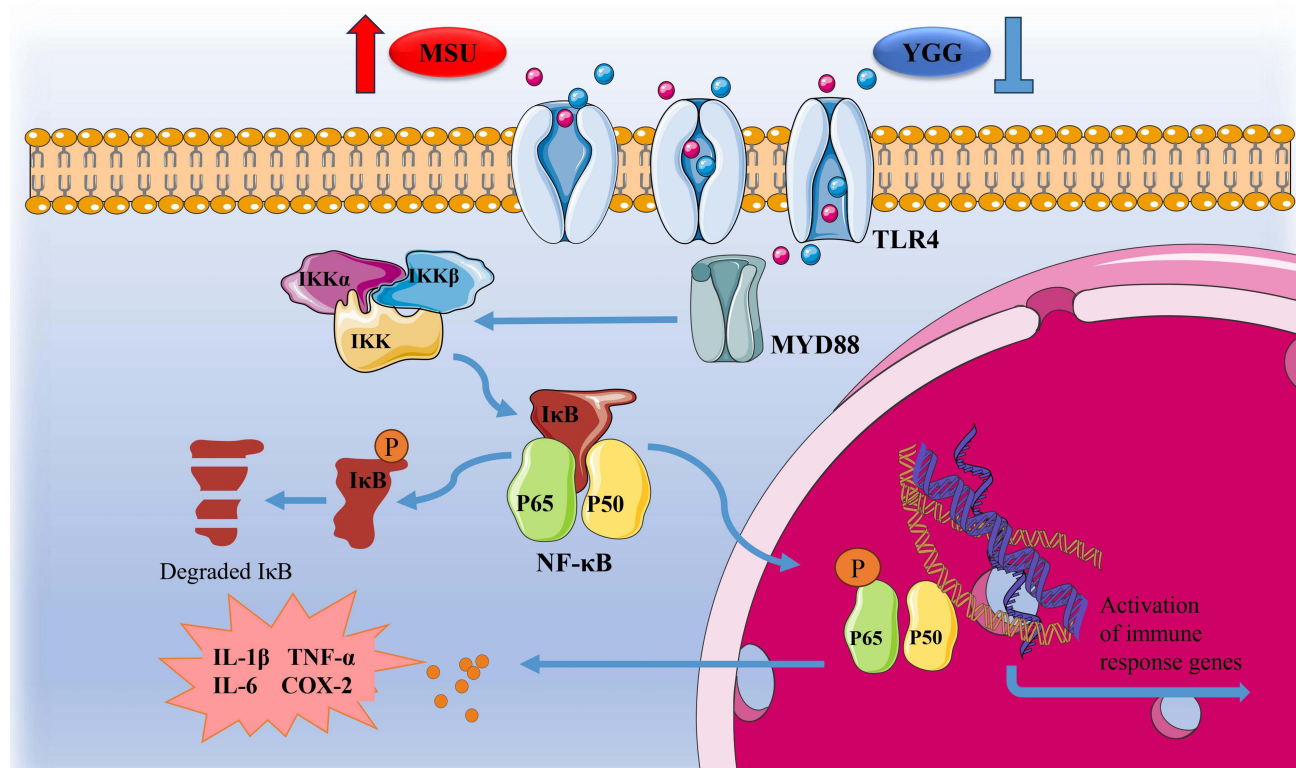


Figure 11 The mechanisms of YGG on GA induced by MSU.

Conclusion

In this study, UPLC-ESI-MS/MS and network pharmacology studies were used to screen 10 major active components of YGG. Animal experiments have shown that YGG can reduce the level of UA in vivo by inhibiting the activity of XO on the one hand, and alleviate the inflammatory response caused by GA by inhibiting the expression of COX-2, PGE2 and inflammatory factors on the other hand. In addition, by integrating transcriptomic and network pharmacology approaches and validation experiments, we confirmed that YGG could regulate TLR4/MYD88/NF- κ B signaling pathway to achieve effective treatment of GA. In conclusion, this study not only provides a basis for studying the active components and mechanism of action of YGG in the treatment of GA, but also provides theoretical support for its clinical application and further strengthens the reliability of YGG clinical application. At the same time, this study also provides reliable candidate components for future drug development for the treatment of GA.

Abbreviations

YGG, Yinhua Gout Granules; GA, Gouty arthritis; HUA, Hyperuricemia; TCM, traditional Chinese medicine; PO, Potassium oxonate; UA, Uric acid; Cr, Creatinine; BUN, Blood urea nitrogen; XO, Xanthine oxidase; BP, Biological processes; MF, Molecular functions; CC, Cellular components; IHC, immunohistochemical.

Data Sharing Statement

The data that support the findings of this study are available from the corresponding author, [Dongyan-Guo, Huan Tian], upon reasonable request.

Ethical Statement

All experiments, including experimental manipulation and animal euthanasia, were authorized by Shaanxi University of Traditional Chinese Medicine's Animal Ethics Committee and strictly operated according to the Guide for the Care and Use of Laboratory Animals published by the US National Institutes of Health, strictly abide by the "Five F" and the "Three R" principle. (License no. SUCMDL 20220605001)

Acknowledgments

This research was supported by grants from Natural Science Basic Research Program Project of Shaanxi Province (grant number 2022JQ-817), Open Project of Shaanxi Key Laboratory of Chinese Medicine Fundamentals and New Drugs Research (grant number KF2201). The Disciplinary Innovation Team Construction Project of Shaanxi University of Chinese Medicine (grant number 2019-YL11).

Author Contributions

All authors made a significant contribution to the work reported, whether that is in the conception, study design, execution, acquisition of data, analysis and interpretation, or in all these areas; took part in drafting, revising or critically reviewing the article; gave final approval of the version to be published; have agreed on the journal to which the article has been submitted; and agree to be accountable for all aspects of the work.

Disclosure

The authors declare that there are no conflicts of interest.

References

1. Huang CY, Chang YY, Chang ST, Chang HT. Xanthine oxidase inhibitory activity and chemical composition of Pistacia chinensis leaf essential oil. *Pharmaceutics*. 2022;14(10):1982. doi:10.3390/pharmaceutics14101982
2. Zhang CL, Zhang JJ, Zhu QF, et al. Antihyperuricemia and antigouty arthritis effects of Persicaria capitata herba in mice. *Phytomedicine*. 2021;93:153765. doi:10.1016/j.phymed.2021.153765
3. Li H, Zhang X, Gu L, et al. Anti-gout effects of the medicinal fungus phellinus igniarius in hyperuricaemia and acute gouty arthritis rat models. *Front Pharmacol*. 2021;12:801910. doi:10.3389/fphar.2021.801910

4. Xiao N, Qu J, He S, et al. Exploring the therapeutic composition and mechanism of jiang-suan-chu-bi recipe on gouty arthritis using an integrated approach based on chemical profile, network pharmacology and experimental support using molecular cell biology. *Front Pharmacol.* 2019;10:1626. doi:10.3389/fphar.2019.01626
5. Becker MA, Fitz-Patrick D, Choi HK, et al. An open-label, 6-month study of allopurinol safety in gout: the LASSO study. *Semin Arthritis Rheum.* 2015;45(2):174–183. doi:10.1016/j.semarthrit.2015.05.005
6. Wilson L, Saseen JJ. Gouty arthritis: a review of acute management and prevention. *Pharmacotherapy.* 2016;36(8):906–922. doi:10.1002/phar.1788
7. Bai L, Wu C, Lei S, et al. Potential anti-gout properties of Wuwei Shexiang pills based on network pharmacology and pharmacological verification. *J Ethnopharmacol.* 2023;305:116147. doi:10.1016/j.jep.2023.116147
8. Li C, Wang C, Guo Y, et al. Research on the effect and underlying molecular mechanism of Cangzhu in the treatment of gouty arthritis. *Eur J Pharmacol.* 2022;927:175044. doi:10.1016/j.ejphar.2022.175044
9. Liu Q, Li L, Zheng D, et al. Mechanism of ShuiJingDan in treating acute gouty arthritis flares based on network pharmacology and molecular docking. *Drug Des Devel Ther.* 2023;17:3493–3505. doi:10.2147/dddt.S436360
10. Cao YX, Ji P, Wu FL, et al. Lonicerae Japonicae Caulis: a review of its research progress of active metabolites and pharmacological effects. *Front Pharmacol.* 2023;14:1277283. doi:10.3389/fphar.2023.1277283
11. Wang S, Liu W, Wei B, et al. Traditional herbal medicine: therapeutic potential in acute gouty arthritis. *J Ethnopharmacol.* 2024;330:118182. doi:10.1016/j.jep.2024.118182
12. Chen LX, Liang W. The research progress of figwort chemical components and pharmacological activities. *Specialty Res.* 2023;45(01):147–151. doi:10.16720/j.cnki.tcyj.2023.010
13. Bai XL, Pei RX, Zhang JL, et al. Curative effect of Yinhuo Gout granules in the treatment of damp-heat accumulated gouty arthritis. *Shaanxi J Tradit Chin Med.* 2018;39(4):494–496.
14. Zhang JL, Pei RX. Observation of curative effect of Yinhuadong granule on type 2 diabetes mellitus complicated with hyperuricemia. *Tradit Chin Med in Western Chin.* 2014;27(01):106–108.
15. Lei W, Zhang ZQ, Yang GC, et al. Regulation of inflammatory factors in patients with acute gout by combination of Yinhuo Gout granules and celecoxib capsules. *Chin Med Innovation.* 2022;19(10):86–89.
16. Luo TT, Lu Y, Yan SK, Xiao X, Rong XL, Guo J. Network pharmacology in research of Chinese medicine formula: methodology, application and prospective. *Chin J Integr Med.* 2020;26(1):72–80. doi:10.1007/s11655-019-3064-0
17. Xiao Y, Liu Y, Lai Z, et al. An integrated network pharmacology and transcriptomic method to explore the mechanism of the total Rhizoma Coptidis alkaloids in improving diabetic nephropathy. *J Ethnopharmacol.* 2021;270:113806. doi:10.1016/j.jep.2021.113806
18. Li JC, Li SY, Song Q, et al. The mechanism of total flavonoids from rattan tea against gouty arthritis was studied based on multi-level interactive network and in vivo experiment. *China J Chin Mater Med.* 2022;47(17):4733–4743. doi:10.19540/j.cnki.cjcm.20220223.701
19. Wang Y, Zou J, Jia Y, et al. The mechanism of lavender essential oil in the treatment of acute colitis based on "quantity-effect" weight coefficient network pharmacology. *Front Pharmacol.* 2021;12:644140. doi:10.3389/fphar.2021.644140
20. Shi G, Kong J, Wang Y, Xuan Z, Xu F. Glycyrrhiza uralensis Fisch. alleviates dextran sulfate sodium-induced colitis in mice through inhibiting of NF- κ B signaling pathways and modulating intestinal microbiota. *J Ethnopharmacol.* 2022;298:115640. doi:10.1016/j.jep.2022.115640
21. Xu GR, Zhang C, Yang HX, et al. Modified citrus pectin ameliorates myocardial fibrosis and inflammation via suppressing galectin-3 and TLR4/MyD88/NF- κ B signaling pathway. *Biomed Pharmacother.* 2020;126:110071. doi:10.1016/j.biopha.2020.110071
22. Zhang W, Huai Y, Miao Z, Qian A, Wang Y. Systems pharmacology for investigation of the mechanisms of action of traditional Chinese medicine in drug discovery. *Front Pharmacol.* 2019;10:743. doi:10.3389/fphar.2019.00743
23. Li WY, Yang F, Chen JH, Ren GF. β -Caryophyllene Ameliorates MSU-Induced Gouty Arthritis and Inflammation Through Inhibiting NLRP3 and NF- κ B Signal Pathway: in Silico and In Vivo. *Front Pharmacol.* 2021;12:651305. doi:10.3389/fphar.2021.651305
24. Yin C, Liu B, Wang P, et al. Eucalyptol alleviates inflammation and pain responses in a mouse model of gout arthritis. *Br J Pharmacol.* 2020;177(9):2042–2057. doi:10.1111/bph.14967
25. Mohapatra A, Rajendrakumar SK, Chandrasekaran G, et al. Biomaterialized nanoscavenger abrogates proinflammatory macrophage polarization and induces neutrophil clearance through reverse migration during gouty arthritis. *ACS Appl Mater Interfaces.* 2023;15(3):3812–3825. doi:10.1021/acsami.2c19684
26. Jiao C, Liang H, Liu L, Li S, Chen J, Xie Y. Transcriptomic analysis of the anti-inflammatory effect of Cordyceps militaris extract on acute gouty arthritis. *Front Pharmacol.* 2022;13:1035101. doi:10.3389/fphar.2022.1035101
27. Wen P, Luo P, Zhang B, Zhang Y. Mapping knowledge structure and global research trends in gout: a bibliometric analysis from 2001 to 2021. *Front Public Health.* 2022;10:924676. doi:10.3389/fpubh.2022.924676
28. Lin Y, Luo T, Weng A, et al. Gallic Acid Alleviates Gouty Arthritis by Inhibiting NLRP3 Inflammasome Activation and Pyroptosis Through Enhancing Nrf2 Signaling. *Front Immunol.* 2020;11:580593. doi:10.3389/fimmu.2020.580593
29. Yong T, Liang D, Chen S, et al. Caffeic acid phenethyl ester alleviated hypouricemia in hyperuricemic mice through inhibiting XOD and up-regulating OAT3. *Phytomedicine.* 2022;103:154256. doi:10.1016/j.phymed.2022.154256
30. Yong T, Liang D, Xiao C, et al. Hypouricemic effect of 2,4-dihydroxybenzoic acid methyl ester in hyperuricemic mice through inhibiting XOD and down-regulating URAT1. *Biomed Pharmacother.* 2022;153:113303. doi:10.1016/j.biopha.2022.113303
31. Ma N, Zhang Y, Wang T, Sun Y, Cai S. The preventive effect of Chinese sumac fruit against monosodium urate-induced gouty arthritis in rats by regulating several inflammatory pathways. *Food Funct.* 2023;14(2):1148–1159. doi:10.1039/d2fo02860c
32. Tang N, Dong Y, Chen C, Zhao H. Anisodamine maintains the stability of intervertebral disc tissue by inhibiting the senescence of nucleus pulposus cells and degradation of extracellular matrix via Interleukin-6/Janus Kinases/Signal Transducer and Activator of Transcription 3 Pathway. *Front Pharmacol.* 2020;11:519172. doi:10.3389/fphar.2020.519172
33. Ruiz-Limon P, Ladehesa-Pineda ML, Castro-Villegas MDC, et al. Enhanced NETosis generation in radiographic axial spondyloarthritis: utility as biomarker for disease activity and anti-TNF- α therapy effectiveness. *J Biomed Sci.* 2020;27(1):54. doi:10.1186/s12929-020-00634-1
34. Gao H, Kang N, Hu C, et al. Ginsenoside Rb1 exerts anti-inflammatory effects in vitro and in vivo by modulating toll-like receptor 4 dimerization and NF- κ B/MAPKs signaling pathways. *Phytomedicine.* 2020;69:153197. doi:10.1016/j.phymed.2020.153197

35. Zhang SS, Liu M, Liu DN, Shang YF, Du GH, Wang YH. Network pharmacology analysis and experimental validation of kaempferol in the treatment of ischemic stroke by inhibiting apoptosis and regulating neuroinflammation involving neutrophils. *Int J Mol Sci.* 2022;23(20). doi:10.3390/ijms232012694
36. Zhao L, Zhang H, Li N, et al. Network pharmacology, a promising approach to reveal the pharmacology mechanism of Chinese medicine formula. *J Ethnopharmacol.* 2023;309:116306. doi:10.1016/j.jep.2023.116306
37. Li D, Rui YX, Guo SD, Luan F, Liu R, Zeng N. Ferulic acid: a review of its pharmacology, pharmacokinetics and derivatives. *Life Sci.* 2021;284:119921. doi:10.1016/j.lfs.2021.119921
38. Muvhulawa N, Dlodla PV, Ziqubu K, et al. Rutin ameliorates inflammation and improves metabolic function: a comprehensive analysis of scientific literature. *Pharmacol Res.* 2022;178:106163. doi:10.1016/j.phrs.2022.106163
39. Shen R, Ma L, Zheng Y. Anti-inflammatory effects of luteolin on acute gouty arthritis rats via TLR/MyD88/NF- κ B pathway. *Zhong Nan Da Xue Xue Bao Yi Xue Ban.* 2020;45(2):115–122. doi:10.11817/j.issn.1672-7347.2020.190566
40. Nile SH, Keum YS, Nile AS, Jalde SS, Patel RV. Antioxidant, anti-inflammatory, and enzyme inhibitory activity of natural plant flavonoids and their synthesized derivatives. *J Biochem Mol Toxicol.* 2018;32(1). doi:10.1002/jbt.22002
41. Ajiboye TO, Ajala-Lawal RA, Adeyiga AB. Caffeic acid abrogates 1,3-dichloro-2-propanol-induced hepatotoxicity by upregulating nuclear erythroid-related factor 2 and downregulating nuclear factor-kappa B. *Hum Exp Toxicol.* 2019;38(9):1092–1101. doi:10.1177/0960327119851257
42. Yang BC, Fu XJ, Zhu L. Effect of ziyunin on JNK/p38 MAPK signaling pathway in rats with knee osteoarthritis. *Chin J Osteoporosis.* 2022;28(10):1491–1495+1500.
43. Meng ZQ, Tang ZH, Yan YX, et al. Study on the anti-gout activity of chlorogenic acid: improvement on hyperuricemia and gouty inflammation. *Am J Chin Med.* 2014;42(6):1471–1483. doi:10.1142/s0192415x1450092x
44. Shen Z, Yang C, Zhu P, Tian C, Liang A. Protective effects of syringin against oxidative stress and inflammation in diabetic pregnant rats via TLR4/MyD88/NF- κ B signaling pathway. *Biomed Pharmacother.* 2020;131:110681. doi:10.1016/j.biopha.2020.110681
45. Cai D, Zhang J, Yang J, Lv Q, Zhong C. Overexpression of FTO alleviates osteoarthritis by regulating the processing of miR-515-5p and the TLR4/MyD88/NF- κ B axis. *Int Immunopharmacol.* 2023;114:109524. doi:10.1016/j.intimp.2022.109524
46. Xu X, Li N, Wu Y, et al. Zhuifeng tougu capsules inhibit the TLR4/MyD88/NF- κ B signaling pathway and alleviate knee osteoarthritis: in vitro and in vivo experiments. *Front Pharmacol.* 2022;13:951860. doi:10.3389/fphar.2022.951860
47. Jin S, Guan T, Wang S, et al. Dioscin alleviates cisplatin-induced mucositis in rats by modulating gut microbiota, enhancing intestinal barrier function and attenuating TLR4/NF- κ B signaling cascade. *Int J Mol Sci.* 2022;23(8). doi:10.3390/ijms23084431
48. Han J, Shi G, Li W, Xie Y, Li F, Jiang D. Preventive effect of dioscin against monosodium urate-mediated gouty arthritis through inhibiting inflammasome NLRP3 and TLR4/NF- κ B signaling pathway activation: an in vivo and in vitro study. *J Nat Med.* 2021;75(1):37–47. doi:10.1007/s11418-020-01440-7
49. Luo Z, Yang F, Hong S, et al. Role of microRNA alternation in the pathogenesis of gouty arthritis. *Front Endocrinol.* 2022;13:967769. doi:10.3389/fendo.2022.967769
50. Hu N, Wang C, Dai X, et al. Phillygenin inhibits LPS-induced activation and inflammation of LX2 cells by TLR4/MyD88/NF- κ B signaling pathway. *J Ethnopharmacol.* 2020;248:112361. doi:10.1016/j.jep.2019.112361
51. Chen B, Li H, Ou G, Ren L, Yang X, Zeng M. Curcumin attenuates MSU crystal-induced inflammation by inhibiting the degradation of I κ B α and blocking mitochondrial damage. *Arthritis Res Ther.* 2019;21(1):193. doi:10.1186/s13075-019-1974-z
52. Kawai T, Akira S. Signaling to NF-kappaB by Toll-like receptors. *Trends Mol Med.* 2007;13(11):460–469. doi:10.1016/j.molmed.2007.09.002
53. Chen R, Li F, Zhou K, et al. Component identification of modified sanmiao pills by UPLC-Xevo G2-XS QTOF and its anti-gouty arthritis mechanism based on network pharmacology and experimental verification. *J Ethnopharmacol.* 2023;311:116394. doi:10.1016/j.jep.2023.116394
54. Jin X, He R, Liu J, et al. An herbal formulation "Shenshuifu Granule" alleviates cisplatin-induced nephrotoxicity by suppressing inflammation and apoptosis through inhibition of the TLR4/MyD88/NF- κ B pathway. *J Ethnopharmacol.* 2023;306:116168. doi:10.1016/j.jep.2023.116168

Drug Design, Development and Therapy

Dovepress

Publish your work in this journal

Drug Design, Development and Therapy is an international, peer-reviewed open-access journal that spans the spectrum of drug design and development through to clinical applications. Clinical outcomes, patient safety, and programs for the development and effective, safe, and sustained use of medicines are a feature of the journal, which has also been accepted for indexing on PubMed Central. The manuscript management system is completely online and includes a very quick and fair peer-review system, which is all easy to use. Visit <http://www.dovepress.com/testimonials.php> to read real quotes from published authors.

Submit your manuscript here: <https://www.dovepress.com/drug-design-development-and-therapy-journal>